

Understanding Health Video Engagement: An Interpretable Deep Learning Approach

Jiaheng Xie

University of Delaware jxie@udel.edu

Yidong Chai

Hefei University of Technology chaiyd@hfut.edu.cn

Xiao Liu

Arizona State University xiao.liu.10@asu.edu

Please send comments to Jiaheng Xie at jxie@udel.edu

*WITS 2021 Best Paper Award Winner

Understanding Health Video Engagement: An Interpretable Deep Learning Approach

Abstract: Predicting video engagement is a top priority for content creators and video-sharing platforms. Early assessment of video popularity enables content creators to maximize their influences and optimize video production budgets. Video sharing platforms also disclosed that they rely on video engagement prediction to promote credible videos and curb violative videos. Deep learning has been deployed to predict video engagement. While achieving state-of-the-art predictive performance, deep learning lacks interpretability. To remedy this gap, we propose a novel interpretable deep learning approach, Generative Adversarial Network-based Piecewise Wide and Attention Deep Learning (GAN-PiWAD), to predict video engagement. Improving upon state-of-the-art interpretable methods, GAN-PiWAD incorporates unstructured data, captures the interactions among multi-modal inputs, offers a precise estimation of the total effect, and models the dynamic total effect when feature value varies. GAN-PiWAD's prediction outperforms strong benchmarks on two use cases: general video engagement prediction and misinformation viewership prediction. Results from a user study confirm that the interpretability of GAN-PiWAD is superior to state-of-the-art interpretable methods. This study contributes to IS with a novel interpretable deep learning framework that is generalizable to understand other human decision factors. Our findings provide direct implications for content creators and video sharing platforms to take proactive actions to improve video engagement and manage video credibility.

Keywords: Interpretable deep learning, video engagement, predictive analytics, user study.

1. Introduction

Social media is increasingly taking up a greater share of consumers' attention and time spent online, and hence becoming an effective and efficient channel to disseminate information and share knowledge. Among various social media platforms, video-sharing sites, such as YouTube and Vimeo, receive the most attention because of their easy-to-implement audio messages, visual presentations to spread information, and extensive viewer base. Video sharing technologies offer promising new venues to disseminate information to wider audiences and make the newest ideas accessible and easy to share.

How does a video become viral? This is one of the well-known open research questions in social

media analytics and the key profit driver for stakeholders of video-sharing sites. Viewership is a key measurement for viewer engagement and is the metric by which platforms pay their content creators (Hoiles et al. 2017, Liu et al. 2020). In this paper, we propose an interpretable machine learning (ML) to predict viewer engagement and interpret the factors associated with engagement. We define viewer engagement as the average daily viewership of a video (Liu et al. 2020). The factors associated with engagement can be used to guide content design and effectively convey public messages in times needed.

Predicting viewer engagement is fundamental to “viralize” videos for these stakeholders. Content creators rely on viewership prediction to boost revenues. Our proposed method is of direct relevance to content creators to better understand and improve consumer engagement. Producing a video costs \$1,500 to \$50,000 per minute (Hinge Marketing 2021). Video production requires novel skills such as shooting and editing, as well as a considerably different communication mindset for elaborate audio-visual storytelling, which average content creators may find difficult to acquire. An interpretable ML viewership prediction helps identify approaches to improve viewer engagement and allocate budgets to potentially popular videos. Advertisers can also greatly benefit from such a prediction. For instance, YouTube adopts the cost-per-view (CPV) model to charge advertisers \$0.06 for each video view (Hubspot 2021). Accurate prediction of video viewership lowers unnecessary advertising costs and optimizes marketing outcomes.

Besides content creators and advertisers, video-sharing sites can benefit from such a prediction. For instance, YouTube is keen to predict video viewership in order to manage video credibility, especially during the COVID-19 pandemic. YouTube hosts more than 100 million videos that provide information on pathogenesis, diagnosis, treatment, and prevention of various medical conditions (Madathil et al. 2015). Although high engagement of credible health videos benefits public health, widely shared health misinformation undermines the global health response and jeopardizes public health education. Health misinformation is detrimental to viewers’ physical and mental health, elevates stigmatization and hate speech, threatens health gains, leads to poor health measures, and even costs lives (WHO 2020). YouTube has revised its guidelines to address misinformation with a range of tools: removing content that violates its policies, raising up authoritative sources for news and information, and reducing recommendations of

borderline content and misinformation. YouTube currently relies on the percentage of total views coming from misinformation videos to prevent them from spreading (NYTimes 2021). Predicting viewership helps the platform increase the views for legitimate videos and curb the views for misinformation videos.

While ML and data-driven approaches present an incredibly potent resource to predict viewer engagement, several challenges have limited the uptake of ML tools. Among them, a lack of transparency and interpretability have been highlighted as significant challenges for wider ML adoption (Linardatos et al. 2020). Interpretability is essential to increase human trust and acceptance of ML models.

Interpretation in the data science life cycle largely occurs in the *post-hoc* analysis and modeling stages (Murdoch et al. 2019). The general principle of these interpretable methods is to estimate the total effect of the prediction, defined as the change of the outcome variable when a feature increases by one unit. Interpretability in the *post-hoc* analysis stage is called *post-hoc* interpretability. *Post-hoc* methods interpret the total effect after the prediction using standalone explaining models, such as regression, sensitivity analyses, SHAP, and LIME (Rafique et al. 2019, Tsang et al. 2018). Although these methods offer cursory explanations to the prediction, the standalone explaining models could alter the total effect of the prediction model, since they possess different model specifications (Guo et al. 2020).

Interpretability in the modeling stage is called model-based interpretability. Model-based methods address the limitation of *post-hoc* models by embedding the interpretable component within the prediction model, so that interpretation and prediction can be made simultaneously. The cutting-edge model-based interpretable methods include the Generalized Additive Model framework (GAM) and the Wide and Deep Learning framework (W&D). GAM is unable to model any higher-order feature interactions and is constrained by the number of features, limiting its applicability in this study. Addressing that, W&D incorporates a linear model in the deep learning model (Cheng et al. 2016). We define the effect interpreted by the linear model (feature weights in the linear model) as the main effect. A few limitations persist for W&D. From the prediction perspective, the W&D framework is restricted to structured data, constrained by the linear part. In video analytics, only using structured data significantly hampers the prediction performance. From the interpretation perspective, W&D and its variants fall short in producing

precise interpretations. They use the weights of the linear part (main effect) to approximate the total effect of the input on the prediction, even though the main effect and total effect largely differ. In addition, W&D and its variants neglect the interactions between the inputs, which is critical in this study. Furthermore, the total effect of a feature on the prediction is dynamic when the feature value varies.

To address the limitations of the existing interpretable methods, we propose a novel model-based interpretable method that leverages unstructured data, captures the interaction effects, produces a precise interpretation, and models the dynamic total effect. Our proposed method is called Generative Adversarial Network-based Piecewise Wide and Attention Deep Learning (GAN-PiWAD). We examine the performance of our method in the context of YouTube health videos due to its broader impact on the well-being of the users, nurturing credible content creation, and the growth of the platform.

This study contributes to data analytics methodology, information systems (IS), and social media analytics. First, we develop GAN-PiWAD that innovatively modifies the W&D framework by incorporating an unstructured component, an attention-based second-order component, and a WGAN-GP component. Empirical evaluations indicate that GAN-PiWAD outperforms the baseline models in two contexts: general health videos and health misinformation videos. GAN-PiWAD also contributes to interpretable ML. We design a user study to quantify the interpretability of interpretable models. The user study indicates GAN-PiWAD provides better interpretability than state-of-the-art interpretable methods. Our feature interpretation enhances decisions and actions via improved trust and model usefulness. This user study serves as an exemplar for IS research to evaluate interpretable ML methods.

Second, for computational IS research (Abbasi et al. 2010, 2012, Fang et al. 2013, Mai et al. 2018, Saboo 2016, Stieglitz and Dang-Xuan 2013), the successful design of our method offers indispensable design principles. Our method development and evaluations prove that capturing the interactions among multi-modal inputs could boost the predictive performance of interpretable methods. Our newly-added deep generative component also offers a generalizable approach to estimate the precise total effect of prediction tasks, as well as the dynamic total effect of each factor. The complex total effect is taken into consideration when the factor value changes. GAN-PiWAD is a generalizable interpretable deep learning

model for many other predictive tasks, such as user engagement prediction, product sales prediction, and project investment prediction. The interpretation of the predictive method sets an exemplar for other design science studies to not only predict an outcome, but offer invaluable interpretability as well.

Third, our findings provide video-sharing sites with practical implications regarding video credibility control. Our method is capable of identifying videos that are on the edge of abruption. Among them, misinformation videos necessitate timely control. To help these platforms design actionable intervention plans, our model interpreted the prediction results. Social media platforms could leverage our method to actively monitor the predictors and prevent the spread of misinformation.

2. Literature Review

2.1. YouTube Viewer Engagement

Our empirical analysis is implemented with YouTube videos. YouTube has been one of the most successful video-sharing sites since its establishment in 2005 and constitutes the largest share of Internet traffic (Richier et al. 2014). Viewership, defined as the number of views a video receives (Szabo and Huberman 2010), is the key metric to measure viewer engagement and by which YouTube pays its content creators (Hoiles et al. 2017).

As YouTube relies on user-generated content, it is constantly bombarded with videos that run afoul of its guidelines, ranging from pornography, copyrighted material, violent extremism, to misinformation. The company has developed its AI system to prevent violative videos from spreading. YouTube recently revealed that this AI system's effectiveness in finding and removing rule-breaking videos is evaluated with a metric called the violative view rate, which is the percentage of total views on YouTube coming from violative videos (NYTimes 2021). This disclosure shows that video view count is considered the most important measure that YouTube seeks to track to increase the view counts for legitimate videos and at the same time to curb the view counts for violative videos.

Understanding and predicting viewership is useful from the content creators' perspective as well. On one hand, more popular content generates more traffic, so understanding viewership has a direct impact on caching and replication strategy that content creators should adopt. On the other hand, viewership has

a direct economic impact, as content creators rely on viewership for payment and advertisement.

2.2. Interpretability Definition and Value Proposition

According to Breiman (2001), ML has two objectives: prediction (determine the value of the target for new inputs) and information (understand the relationship between the inputs and the target). Studies show that decision makers exhibit an inherent distrust of automated predictive models, even if they are proven to be more accurate than human forecasters (Dietvorst et al. 2015). When ML models are used to support decision-making on complex and important topics, understanding a model's "reasoning" can increase trust in its predictions, expose hidden biases, and reduce vulnerability to adversarial attacks. To fully harness the power of AI and ML to support decision-making, interpretability is a much-needed milestone.

The definition of interpretability remains inconclusive, and domain-specific notions are left to the researchers and users to define (Lee et al. 2018). Related to ML and predictive analytics, two major definitions exist. One stream defines interpretability as the degree to which a human can trust and understand the cause of a decision (Miller 2019). In the context of ML, interpretability is described as the degree to which a human can consistently predict the model's result (Miller 2019). The interpretability of a model is higher if it is easier for a person to trust the model and trace back why a prediction was made by the model (Doshi-Velez and Kim 2017). Molnar (2019) notes that interpretable ML refers to models that make the behavior and predictions of ML understandable and trustworthy to humans. Consequently, interpretability is related to how well humans trust a model by looking and reasoning about it. The other stream suggests "AI is interpretable to the extent that the produced interpretation is able to maximize a user's target performance" (Dhurandhar et al. 2017). Following this definition, Lee et al. (2018) uses usefulness to measure ML interpretability, as useful models lead to better decision-making performance.

Interpretability brings value to ML and the business world in many aspects. The most significant one is social acceptance, which is required to integrate algorithms into daily lives. Heider and Simmel (1944) show that people attribute beliefs and intentions to abstract objects, so they are more likely to accept ML if their decisions are interpretable. Ribeiro et al. (2016) argue that if users do not trust a model prediction, they will not use it. Interpretability is thus essential to increase human trust and acceptance of ML.

For human societies to embrace ML for decision support, ML must bring forth relevant information for the decision-making task and communicate in a way that allows a human recipient of the information to establish trust using intuition and reasoning (Varshney et al. 2018). As our society is progressing toward the integration with ML and AI, new regulations have been imposed to require verifiability, accountability, and, more importantly, full transparency of algorithm decisions. A key example is the European General Data Protection Regulation (GDPR), which was enforced to provide data subjects with the right to an explanation of algorithm decisions (Weller 2017).

In the case of viewership prediction for content moderation and production on social media, the transparency of algorithms is critical to avoid arbitrary decisions and backlash from the public about the violation of the Freedom of Speech. In the battle of misinformation, it is beneficial for YouTube and content creators to understand factors associated with popularity and build trust in certain systems so that patterns of misinformation spread can be learned, and that harmful content can be removed. For viewers, trust leads to better customer adherence on the platform and more content consumption. For credible content creators, especially healthcare organizations and news sources that share valuable knowledge and evidence-based information, it takes significant time and effort to create such content. Interpretable predictions of viewer engagement can also guide them to create more high-quality and compelling content that may gain high viewer engagement.

2.3. Interpretable Machine Learning Methods

Recent video analytics studies heavily utilize deep learning models (Arinaldi et al. 2018, Yaseen et al. 2019). Although these models pioneer predictive analytics, their lack of interpretability fails to provide actionable insights for business decision-making. To remedy this gap, we propose an interpretable deep learning approach. We develop a taxonomy of the extant interpretable methods based on the data types that these methods deal with, the type of algorithms that could be applied (i.e., model-based and *post-hoc*), the scope of interpretation (i.e., instance level and model level), and how they attempt to address interpretability. Table 1 summarizes these interpretable methods.

Table 1. Summary of Recent Work in Interpretable Machine Learning Methods

Model	Scope	Data Type	Interpretable Method	Usage
Deconvolutional Nets (Zeiler & Fergus 2014)	Instance-level	Image	Backpropagation	Post-hoc
GAM (Caruana et al. 2015)	Model-level	Tabular	GAM	Model-based
LIME (Ribeiro et al. 2016)	Both	Any	Perturbation	Post-hoc
W&D (Cheng et al. 2016)	Model-level	Tabular	W&D	Model-based
SHAP (Lundberg et al. 2017)	Both	Any	Perturbation	Post-hoc
Grad-CAM (Selvaraju et al. 2017)	Instance-level	Image	Backpropagation	Post-hoc
Focused Concept Miner (Lee et al. 2018)	Both	Text	Topic Model	Model-based
W&D-CNN (Lee and Chan 2019)	Model-level	Tabular	W&D	Model-based
W&D-BLSTM (Ye et al. 2019)	Model-level	Tabular	W&D	Model-based
CaCE (Goyal et al. 2019)	Model-level	Image	GAM	Post-hoc
LRP (Montavon et al. 2019)	Both	Any	Backpropagation	Post-hoc
W&D-LSTM (Tosun et al. 2020)	Model-level	Tabular	GAM	Model-based
Piecewise W&D (Guo et al. 2020)	Model-level	Tabular	W&D	Model-based
NAM (Agarwal et al. 2020)	Model-level	Any	GAM	Model-based
Our proposed method	Both	Any	W&D + GAN	Model-based

Interpretable ML methods have been developed to discover, learn, and extract the hierarchical representations needed for prediction tasks. One crucial factor that should be considered is the data type to which these methods could be applied. Vast amounts of data in various forms have been used to train and develop such methods, including tabular (Guo et al. 2020, Tosun et al. 2020), image (Goyal et al. 2019, Selvaraju et al. 2017), and text (Agarwal et al. 2020, Lee et al. 2018).

The scope of an interpretable method depends on whether it interprets a local instance or understands the model as a whole. The scope of interpretations can be either instance- or model-level. Locally interpretable methods are designed to express the individual feature attributions of a single instance of input data (Selvaraju et al. 2017, Zeiler and Fergus 2014). Globally interpretable models provide insights into the decision as a whole – leading to an understanding of attributions for an array of input data (Agarwal et al. 2020, Tosun et al. 2020). Some methods can be extended to both (Lundberg et al. 2017).

An interpretable ML method with a specific scope and methodology can be either embedded in the neural network or applied as an external algorithm for interpretation (Das and Rad 2020). *Post-hoc* methods build on the predictions of an existing neural network and add *ad-hoc* explanations (Goyal et al. 2019, Selvaraju et al. 2017). Any interpretable ML algorithm that is dependent on the model architecture falls into the model-based category (Agarwal et al. 2020, Caruana et al. 2015, Guo et al. 2020). For most model-based algorithms, any change in the architecture needs alteration in the method itself or hyperparameters of the interpretable algorithm. However, model-based interpretable ML methods can better capture dynamic feature effects, higher-order relations of the features, or even interaction effects.

Post-hoc interpretable methods can be categorized into backpropagation-based or perturbation-based (Das and Rad 2020). Interpretations generated by iteratively probing a trained ML model with different inputs fall under perturbation-based techniques. These perturbations can be on the feature level by replacing certain features by zero or random counterfactual instances, picking one or a group of pixels (superpixels) for explanation, blurring, shifting, masking operations, among others.

The Local Interpretable Model-agnostic Explanations (LIME) is one of the most popular *post-hoc* methods (Ribeiro et al. 2016) using the perturbation-based approach. For any given instance and its corresponding prediction, simulated randomly sampled data around the neighborhood of the input instance, for which the prediction was produced, are generated. New predictions are made for generated instances and weighted by their proximity to the input instance. A simple, interpretable model, such as a decision tree, is trained on this newly created dataset of perturbed instances. By interpreting this local model, the initial black-box model is consequently interpreted.

Shapley Additive Explanations (SHAP) has a similar method of probing feature correlations by removing features in a game-theoretic framework (Lundberg et al. 2017). SHAP explains predictions of an input by computing individual feature contributions towards that output prediction. By formulating the data features as players in a coalition game, Shapley values can be computed to learn to distribute the payout fairly. SHAP can deduce the problem where the explanation is a linear function of features.

The other common approach among *post-hoc* interpretable methods is based on backpropagation. The core algorithmic logic is dependent on gradients that are backpropagated from the output layer back to the input layer. Deconvolutional Nets (Zeiler et al. 2013) uses backpropagation for activation visualizations and gives relative importance to gradient value during backpropagation. With Rectified Linear Unit (ReLU) activation, a backpropagation on traditional CNNs would result in zero values for negative gradients, while in Deconvolutional Nets, the gradient value is not clipped at zero. This allowed for accurate visualizations. The Layer-wise Relevance BackPropagation (LRP) technique in Bach et al. (2015) is used to find relevance scores for individual features in the input data by decomposing the output predictions of the DNN. The relevance score to the output class for each instance is calculated by

backpropagating the class scores of an output class node towards the input layer.

While these *post-hoc* methods offer a simplistic form of explainability, the precision of such explainability remains questionable. Zafar and Khan (2019) reported that the random perturbation and feature selection methods that SHAP or LIME utilizes result in unstable generated interpretations. This is because, for the same prediction, different interpretations can be generated, which can be problematic for deployment. The *post-hoc* explaining model is also independent of the prediction model, each possessing unique training objectives and model specifications. The total effect of the prediction model – defined as the change of the outcome variable when a feature increases by one unit – could differ significantly from that learned from the explaining model (Guo et al. 2020). Therefore, the magnitude and direction of the total effect could be misinterpreted by the explaining model.

The model-based interpretable methods have a self-contained structure that not only makes accurate predictions with a single objective function but also can more precisely characterize the relationship between the input features and the outcome. The model-based interpretable methods are usually based on two frameworks: Generalized Additive Model framework (GAM) and Wide and Deep Learning framework (W&D). Caruana et al. (2015) introduced GAMs with pairwise interactions (GA2Ms) to improve the accuracy while maintaining the interpretability of GAMs. However, for prediction tasks with many features, GAMs often require millions of decision trees to provide accurate results using additive algorithms. Also, depending on the model architecture, over-regularization reduces the accuracy of GAM. Numerous methods have improved GAMs. Neural Additive Models (NAM) learn a linear combination of neural networks where each attends to a single input feature: each feature is parametrized by a neural network (Agarwal et al. 2020). These networks are trained jointly and can learn arbitrarily complex shape functions. Interpreting NAMs is easy as the impact of a feature on the prediction does not rely on other features and can be understood by visualizing its corresponding shape function. However, this class of methods is limited in modeling any higher-order feature interactions and is constrained by the number of features, because every single feature is assumed independent and trained by a standalone model. When the number of features is large, and the feature interactions and higher effects exist, the GAMs and NAMs

struggle to perform well (Agarwal et al. 2020).

The W&D framework is explicitly designed to address the low and high-order feature interactions in interpreting the importance of features (Cheng et al. 2016). Cheng et al. (2016) proposed W&D that trains an interpretable linear component jointly with a deep neural network. The wide component is a linear model with the input features. This wide component produces a weight for each feature (main effect) to interpret the prediction. The second joint component is a deep neural network that models high-order relations in the hierarchical network to improve prediction accuracy.

Since the introduction of W&D, a range of its variants have emerged. They fall into two categories. The first category attempts to improve the predictive power of W&D. Since the deep component offers the core predictive capability in W&D, studies in this category design new networks to replace the deep network, such as CNN, CRF, and attention mechanisms. Burel et al. (2017) leveraged CNN in the deep component to identify information categories in crisis-related posts in social media. Instead of feeding separate inputs to the wide and deep components, Guo et al. (2018) developed a shared input layer so that both wide and deep components can share inputs without feature engineering. Han et al. (2019) used a CRF layer to merge the wide and deep components and predict named entities of words. Zhang et al. (2020) designed an attention mechanism to capture the sparse information in health data.

The second category of variants aims to improve the interpretability of W&D. They attempt to tease out the influence of the deep component on the wide component so that the interpretation error from the wide component is mitigated. Guo et al. (2020) proposed piecewise W&D that divides the input features into smaller granularities for piecewise linear approximation. Multiple regularizations are introduced to the total loss function to reduce the influence of the deep component on the wide component so that the weights learned from the wide component are closer to the actual total effect.

The W&D and its variants still fall short in the following aspects. First, unstructured data are not compatible with the W&D framework. The existing W&D framework enforces the wide component and the deep component to share inputs and be trained jointly, so that the wide component can interpret the deep component. Since the wide component can only take structured data, many other data types

described in Table 1, such as videos in this study, are not applicable in W&D, thus significantly limiting its predictive performance in unstructured data analytics.

Second, W&D could only interpret first-order relationships between the input and the output via the wide component. Although some variants attempted to model complex relationships using other networks, the interactions among the features are neglected. The media richness theory suggests that multiple presentation modes and their interactions are essential to model human decision-making (Lengel and Daft 1988). Lim and Benbasat (2002) suggest that multiple input modalities and their interactions could facilitate explanative processing information, such as information concerning relationships between or functions underlying descriptive information. Our study aims to predict and understand viewer engagement using multiple data modalities, including video, audio, and text. Modeling the data interactions needs to be an integral part of the method. For instance, video features and audio features could interact because good visual presentation helps understand audio messages.

Third, when training the wide and deep components jointly, the deep component affects the weights in the wide component during backpropagation. Consequently, the learned weights of the wide component (main effect) are not the total effect. Using those weights to interpret the prediction introduces errors induced by the deep component. Even though a few studies (e.g., Guo et al. 2020) attempted to minimize such errors, their efforts still fail to interpret the precise total effect.

Fourth, existing methods only estimate a constant total effect, assuming the total effect is insensitive to changes of feature value. This assumption does not hold in real settings. For instance, when a video is only a few minutes long, increasing one minute in duration would significantly impact its viewership. When a video is hours long, increasing one minute does not have a visible effect on its viewership.

2.4. Generative Models for Synthetic Sampling

The state-of-the-art interpretable methods, such as the W&D framework, cannot capture the precise total effect. In order to calculate the true total effect, we develop a novel model-based interpretation approach, which we will detail in the Proposed Approach section. To facilitate such an approach, generating synthetic samples to learn the data distribution is essential.

Deep generative models define distributions over a set of variables organized in multiple layers. Early forms of such models dated back to works on Bayesian Networks (Neal 1992) and neural network models such as Helmholtz machines (Dayan et al. 1995). Such models are trained via an EM framework, using either variational inference (Jordan et al. 1999) or data augmentation (Tanner and Wong 1987). Bayesian Networks require the knowledge of the dependency between every feature pair. It would be useful for cases with limited features that have domain knowledge. When the number of features increases, constructing the feature dependencies is infeasible and leads to poor performance.

Recent years have seen a resurgence of developments in deep generative models. The emerging approaches, including Variational Autoencoders (VAEs) (Kingma and Welling 2013) and Generative Adversarial Networks (GANs) (Goodfellow et al. 2014) have led to impressive results in various applications, such as image and text generation (Hu et al. 2017) and disentangled representation learning (Chen et al. 2016). Unlike Bayesian Networks, deep generative models do not require the knowledge of feature dependencies. GANs and VAEs are two emerging families of generative model learning and have been largely considered as two distinct paradigms. VAE aims at maximizing the lower bound of the data log-likelihood, while GAN aims at achieving an equilibrium between Generator and Discriminator.

VAEs use the architecture of autoencoders to learn a data generating distribution (Kingma and Welling 2013). The encoder takes random samples and compresses them into a low-dimensional latent space. The decoder takes the latent space representation and reproduces the original sample. VAE uses variational inferences to generate its approximation to a posterior distribution. Once the VAE is trained, it can generate unique samples that have similar characteristics to those that the network was trained on.

GANs are a powerful class of deep generative models consisting of two networks: a generative network (generator) and a discriminative network (discriminator). These two networks form a contest where the generator produces high-quality synthetic data to fool the discriminator, and the discriminator distinguishes the generator's output from the real data. Through recurrent learning from this contest, the generator is capable of approximating the distribution of the real data. Deep learning literature suggests that the generator could learn the precise real data distribution as long as those two networks are

sufficiently powerful (Goodfellow et al. 2016). The contest between the discriminator and the generator is achieved by training jointly. The resulting model is a generator that can closely approximate the real distribution. This generator can generate samples to compute the precise total effect.

Although both VAE and GANs are very exciting approaches to learn the underlying data distribution using unsupervised learning, GANs yield better results than VAEs empirically (Alqahtani et al. 2021). VAE optimizes the lower variational bound, whereas in GAN there is no such assumption. In fact, GANs do not deal with any explicit probability density estimation. The requirement of VAE to learn explicit density estimation hinders the model’s ability to learn the true posterior distribution.

3. The Proposed Approach

3.1. Problem Definition

Let \mathbf{V} denote a set of videos (v_1, \dots, v_N) . We design M features $\mathbf{X} = (X_1, \dots, X_M)$ to represent each video. The feature values of a video v_i are represented by a vector $\mathbf{x}_i = (x_{i,1}, \dots, x_{i,M})$. We also leverage the raw videos (v_1, \dots, v_N) as the unstructured input. The viewer engagement is operationalized as the average daily views of a video (ADV) (Liu et al. 2020), computed as the view counts to date divided by the number of days a video has been published. The average operation is the average daily views over the entire lifespan of a video. The ADV value of video v_i is denoted as adv_i . Our objective is to learn a model F to predict adv_i , where $adv_i = F(\mathbf{x}_i, v_i)$. In addition to predicting ADV , this model is capable of interpreting how it makes such a prediction. Specifically, our second objective is to refine model F , so that it can estimate the precise total effect of each feature X_j on the output adv ($\Delta ADV/X_j$).

3.2. The Interpretable Deep Learning Approach for Viewer Engagement Prediction

The proposed method extends the state-of-the-art interpretable deep learning and addresses four technical challenges: 1) the W&D framework can only process structured data; 2) W&D and its variants neglect the interactions between multi-modal inputs; 3) extant interpretable models fail to offer a precise total effect; 4) existing interpretable methods do not consider the dynamic total effect when feature value varies. Our proposed method is called Generative Adversarial Network-based Piecewise Wide and Attention Deep

Learning (GAN-PiWAD). The following subsections describe each layer of GAN-PiWAD in detail.

3.2.1. Piecewise Linear Component

Each feature X_j captures a different aspect of a video. Within each feature, heterogeneity between different values exists. For instance, video creator credibility is a feature in \mathbf{X} . Videos with low creator credibility not only influence the outcome variable, but these videos may have low quality as well, which indirectly influences the outcome variable. Therefore, it is essential to consider the homogeneity among similar feature values and the heterogeneity across different feature values. Specifically, we need to differentiate the varied feature effects when the feature is at different values. Consequently, we introduce a piecewise linear function in the linear component. For the j -th feature, let $\beta_j = \max\{x_{i,j} | i = 1, \dots, N\}$ and $\delta_j = \min\{x_{i,j} | i = 1, \dots, N\}$. We partition each feature into γ_j intervals: $[\varphi_j^0, \varphi_j^1], \dots, [\varphi_j^{\gamma_j-1}, \varphi_j^{\gamma_j}]$, where $\varphi_j^k = \delta_j + \frac{k}{\gamma_j}(\beta_j - \delta_j)$. The piecewise feature vector for the i -th data point \mathbf{x}_i is:

$$\Phi_i = (\phi_{i,1}^1, \dots, \phi_{i,1}^{\gamma_1}, \dots, \phi_{i,j}^1, \dots, \phi_{i,j}^{\gamma_j}, \dots, \phi_{i,M}^1, \dots, \phi_{i,M}^{\gamma_M})^T, \quad (1)$$

where $\phi_{i,j}^k = \begin{cases} 1, & x_{i,j} > \varphi_j^k. \\ \frac{x_{i,j} - \varphi_j^{k-1}}{\varphi_j^k - \varphi_j^{k-1}}, & \varphi_j^{k-1} \leq x_{i,j} \leq \varphi_j^k. \\ 0, & \text{otherwise.} \end{cases}$ This piecewise vector Φ_i is then fed into a linear model:

$$y_i^{\text{pw}} = (\mathbf{w}^{\text{pw}})^T \Phi_i + b^{\text{pw}}, \quad (2)$$

where $(\mathbf{w}^{\text{pw}})^T$ is the weight in the piecewise linear component, b^{pw} is the bias, and y_i^{pw} is the output.

3.2.2. Attention-based Second-Order Component

In parallel with the piecewise linear component, we devise an attention-based second-order component to model the interaction effects among the multi-modal features. The input to this component is \mathbf{X} . For each video feature \mathbf{x}_i , the interaction term of $x_{i,j}$ and $x_{i,j'}$ is denoted as $s_{i,(j,j')} = x_{i,j} \cdot x_{i,j'}$. Each interaction term has a parameter (Cheng et al. 2016). A set of M features will generate M^2 interaction terms. This will cause the learnable parameters in the second-order component to grow quadratically as the feature set increases. To prevent such a quadratic growth and optimize computational complexity, we propose a self-attention mechanism in the second-order component where the number of parameters is fixed. The attention-based component could scale to large number of interactions while salient interaction terms still

stand out. The attention mechanism assigns a score $a_{i,(j,j')}$ to each interaction term $s_{i,(j,j')}$.

$$a_{i,(j,j')} = \frac{\exp(u_{i,(j,j')} \cdot h^A)}{\sum_{j=1, j'=1}^{M,M} \exp(u_{i,(j,j')} \cdot h^A)}, \quad (3)$$

$$u_{i,(j,j')} = \tanh(w^A \cdot s_{i,(j,j')} + b^A), \quad (4)$$

where w^A , b^A and h^A are learnable parameters. The number of w^A , b^A and h^A are fixed, thus facilitating the analysis of a large scale of interaction terms. The attention score $a_{i,(j,j')}$ is then used to weigh the interaction terms. The output of the attention-based second-order component is given by

$$y_i^{\text{as}} = w^{\text{as}} \sum_j^M \sum_{j'}^M a_{i,(j,j')} s_{i,(j,j')}, \quad (5)$$

where w^{as} is a learnable weight and $\sum_j^M \sum_{j'}^M a_{i,(j,j')} s_{i,(j,j')}$ is the weighted sum of interaction terms.

3.2.3. Nonlinear Higher-Order Component

The third parallel component is the nonlinear higher-order component. This component is a deep neural network that could capture higher-order effects. This network contains multiple fully connected layers. The number of hidden layers is determined using a grid search in the empirical analyses. The purpose of the higher-order component is to leverage the superior predictive power of deep learning to improve predictability. Different from the dynamic total effect described above, the higher-order effect is a hidden component that is not interpretable, but only serves the predictive purpose. The dynamic total effect is able to delineate the magnitude of each feature's total effect at each feature value. Without loss of generality, for the i -th video, each hidden layer computes:

$$\mathbf{a}_{i,(l+1)} = f(\mathbf{W}_{(l)}^{\text{nh}} \mathbf{a}_{i,(l)} + \mathbf{b}_{(l)}^{\text{nh}}), \quad (6)$$

where l is the layer number. f is the ReLU. $\mathbf{a}_{i,(l)}$, $\mathbf{b}_{(l)}^{\text{nh}}$, and $\mathbf{W}_{(l)}^{\text{nh}}$ are the input, bias, and weight at the l -th layer. As no categorical features are involved in our study, no embedding layer is employed. Therefore, the input of the first layer is the feature vector (i.e., $\mathbf{a}_{i,(1)} = \mathbf{x}_i$). The output of this component is given by

$$y_i^{\text{nh}} = (\mathbf{w}^{\text{nh}})^{\text{T}} \mathbf{a}_{i,(L+1)}, \quad (7)$$

where $(\mathbf{w}^{\text{nh}})^{\text{T}}$ is the learnable weight and L is the number of layers.

3.2.4. Unstructured Component

The W&D framework enforces the wide part and the deep part to share inputs so that the wide part can interpret the deep part. Since the wide part can only analyze structured data, the W&D framework is restricted to structured data as well. However, videos are in an unstructured format by nature. Although feature engineering can be deployed to extract structured features from videos, obtaining high predictive power in video analytics demands the capacity to process unstructured data. Since we do not rely on the main effect for interpretation, we extend the W&D framework with an unstructured component as the fourth parallel processing module. Unlike W&D, this unstructured component does not share input with the other components. It directly takes the raw videos as the input. This component adopts the popular CNN-LSTM architecture for processing videos. We leverage the VGG-16 architecture to process the video frames (Simonyan and Zisserman 2015), and an LSTM model is added on the top for frame-by-frame sequence processing. We denote the component parameter as \mathbf{w}^{uc} , consisting of \mathbf{w}^{CNN} and \mathbf{w}^{LSTM} . The last LSTM cell summarizes the video content information and is denoted as y_i^{uc} for the i -th video v_i .

3.2.5. Wasserstein GAN with Gradient Penalty Layer

In addition to accurately predicting viewer engagement, we aim to estimate the total effect. GAN-PiWAD predicts the outcome variable using

$$\widehat{ADV} = \text{ReLU}(\beta + \alpha_1 X_1 + \dots + \alpha_M X_M + S(X_1, \dots, X_M) + H(X_1, \dots, X_M) + U(v)), \quad (8)$$

where $\beta + \alpha_1 X_1 + \dots + \alpha_M X_M$ denotes the main effect, $S(X_1, \dots, X_M)$ denotes the second-order effect, $H(x_1, \dots, x_n)$ denotes the nonlinear higher-order effect, and $U(v)$ denotes the unstructured effect. We use ReLU because video views are non-negative. The total effect of X_1 equals to the change of \widehat{ADV} when X_1 increases by one unit. In order to model the dynamic total effect of each feature, we predict the total effect of each feature at every value. Let $\widehat{ADV}(X_1 = c)$ denote the expected prediction conditioned on $X_1 = c$.

The dynamic total effect of X_1 under the condition of $X_1 = c$ is given by

$$\begin{aligned} \Delta \widehat{ADV}(X_1 = c | X_2, \dots, X_M) &= \text{ReLU}(\beta + \alpha_1(c + 1) + \dots + \alpha_M X_M + S(X_1 = c + 1, \dots, X_M) + H(X_1 = c + 1, \dots, X_M) + U(v)) \\ &\quad - \text{ReLU}(\beta + \alpha_1 c + \dots + \alpha_M X_M + S(X_1 = c, \dots, X_M) + H(X_1 = c, \dots, X_M) + U(v)). \end{aligned} \quad (9)$$

The variable of interest is X_1 . Therefore, the dynamic total effect of X_1 is computed as

$$\begin{aligned} \Delta \widehat{ADV}(X_1 = c) &= \Delta \mathbb{E}_{X_2, \dots, X_M, v} \widehat{ADV}(X_1 = c, X_2, \dots, X_M, v) \\ &= \Delta \int \dots \int_{X_2, \dots, X_M, v} \widehat{ADV}(X_1 = c, X_2, \dots, X_M, v) p(X_1 = c, X_2, \dots, X_M, v) d(X_2) \dots d(X_M) d(v). \end{aligned} \quad (10)$$

However, Equation 10 is intractable because of the integral computation. In order to facilitate the computation of Equation 10, we utilize the Monte Carlo method. Equation 10 can be transformed to:

$$\Delta \widehat{ADV}(X_1 = c) \approx \frac{1}{K} \sum_{k=1}^K \widehat{ADV}(x_{k,1} = c, x_{k,2}, \dots, x_{k,M}, v), \quad (11)$$

where $(x_{k,1} = c, x_{k,2}, \dots, x_{k,M}, v)$ denotes the k -th sample drawn from the distribution $p(X_1 = c, X_2, \dots, X_M, v)$. The total effect of X_1 varies as the value of X_1 changes. For visualization purposes, we also compute the average total effect of X_1 that averages over the total effects of X_1 during the value range of X_1 . Assume that X_1 ranges from c_{\min} to c_{\max} , the average total effect of X_1 is estimated as

$$\Delta \widehat{ADV}(X_1) = \frac{1}{c_{\max} - c_{\min}} \left(\Delta \widehat{ADV}(X_1 = c_{\max}) - \Delta \widehat{ADV}(X_1 = c_{\min}) \right). \quad (12)$$

In order to compute the precise total effect of X_1 , it is necessary to learn the distribution $p(X_1 = c, X_2, \dots, X_M, v)$, so that samples can be drawn from it. The standard W&D cannot provide a precise total effect. The standard models use the main effect from the linear part to interpret the total effect. However, the change of each feature influences the prediction from both the wide part and the deep part. Therefore, the main effect differs from the total effect (empirically examined in Table 7). We proposed a new method for a precise estimation. As described above, the complexity and intractability of $p(X_1 = c, X_2, \dots, X_M, v)$ hinder the learning of the data distribution. X_1, X_2, \dots, X_M are human-engineered features from six data sources. They reflect the overall characteristics of a YouTube video webpage. v reflects the unstructured raw videos. Therefore, we compute $p(X_1 = c, X_2, \dots, X_M, v)$ as $p(X_1 = c, X_2, \dots, X_M)p(v)$. $p(v)$ can be learned from the research corpus data distribution. However, X_1, X_2, \dots, X_M are numeric data that are sparse when using Monte Carlo method. In order to learn a smooth and accurate distribution, we modify W&D by integrating a generative adversarial network (GAN) to learn $p(X_1 = c, X_2, \dots, X_M)$. To overcome the learning instability issues of GANs, we introduce the Wasserstein GAN with gradient penalty (WGAN-GP) in this study (Gulrajani et al. 2017). We cohesively integrate WGAN-GP in GAN-PiWAD. The learning loss of the discriminator (critic) in our proposed method is given by

$$L_d = \mathbb{E}_{\tilde{x} \sim \mathbb{P}_g} [D(\tilde{x})] - \mathbb{E}_{x \sim \mathbb{P}_r} [D(x)] + \lambda \mathbb{E}_{\hat{x} \sim \mathbb{P}_{\hat{x}}} [(\|\nabla_{\hat{x}} D(\hat{x})\|_2 - 1)^2], \quad (13)$$

where $D(\cdot)$ is a score that measures the quality of the input sample. \mathbb{P}_r is the real distribution. \mathbb{P}_g is the learned distribution by the generator. \hat{x} is sampled uniformly along the straight lines between pairs of points sampled from \mathbb{P}_r and \mathbb{P}_g . The distribution of \hat{x} is denoted as $\mathbb{P}_{\hat{x}}$. $\mathbb{E}_{\hat{x} \sim \mathbb{P}_{\hat{x}}} [(\|\nabla_{\hat{x}} D(\hat{x})\|_2 - 1)^2]$ is the gradient penalty. λ is a positive scalar to control the degree of the penalty. The loss of the generator is:

$$L_g = -\mathbb{E}_{x \sim \mathbb{P}_g} [D(\tilde{x})]. \quad (14)$$

The contest between the discriminator and the generator is achieved by training Equations 13 and 14 jointly. The resulting model of this layer is a generator whose \mathbb{P}_g closely approximates the real distribution \mathbb{P}_r . This generator can generate samples to compute the precise total effect and dynamic total effect according to Equations 8-12.

3.2.6. Joint Training of GAN-PiWAD

The piecewise linear component, attention-based second-order component, nonlinear higher-order component, and unstructured component are trained jointly. The combined model aims to predict:

$$\widehat{adv}_i = f(y_i^{\text{pw}} + y_i^{\text{as}} + y_i^{\text{nh}} + y_i^{\text{uc}}), \quad (15)$$

where \hat{y}_i is the prediction, and $f(\cdot)$ is the ReLU activation function. The joint model is trained according to the mean squared error (MSE). The joint training is performed by backpropagating the gradients from the outputs of all the four components using mini-batch stochastic optimization. After the model is trained, the prediction will be made for an unseen sample and the total effect and the dynamic total effect of each input feature can be calculated. The model includes two sets of parameters: parameters of GAN $\theta_{\text{GAN}} = (\theta_{\text{disc}}, \theta_{\text{gen}})$ and the parameters of PiWAD $\theta_{\text{PiWAD}} = (\mathbf{w}^{\text{pw}}, b^{\text{pw}}, w^{\text{A}}, b^{\text{A}}, h^{\text{A}}, w^{\text{as}}, \mathbf{W}_{(1)}^{\text{nh}}, \mathbf{W}_{(L)}^{\text{nh}}, \mathbf{b}_{(1)}^{\text{nh}}, \mathbf{b}_{(L)}^{\text{nh}}, \mathbf{w}^{\text{nh}}, \mathbf{w}^{\text{uc}})$.

3.2.7. Medical Knowledge Extraction

In this study, we examine GAN-PiWAD in health videos due to its broader societal impact. The proprietary characteristic of these videos is the medical knowledge embedded in the videos. Studies show that medical knowledge is a critical factor that influences viewer engagement of health videos (Liu et al.

2020). We, therefore, incorporate medical knowledge as domain knowledge in our model.

Medical knowledge can be operationalized as the number of medical terms in the video transcript and description (Liu et al. 2020). In order to extract the medical terms from transcripts and descriptions, we leverage the widely adopted entity extraction method Bidirectional Long Short-Term Memory (BLSTM). UMLS is used as a reference for medical term annotation. Consumer health vocabulary (CHV) is used to complement the existing framework of UMLS to connect informal, layperson words, and phrases about health to medical terms used by health professionals. A total of 5,000 sentences are selected from the video description texts for annotation. Usage of medical terms in consumer vocabulary or standard medical format in these sentences are identified by referencing UMLS and CHV by two graduate research associates. The inter-rater reliability for annotating medical terms is 0.87.

Figure 1 details the GAN-PiWAD algorithm. Figure 2 shows its architecture. As indicated in the empirical analyses, our model uses 3 hidden layers with 16 neurons each in the higher-order component. In total, our model has 45,993,706 parameters.

<p>Input: training data that include video features $\mathcal{X}^{\text{tr}} = \{\mathbf{x}_1^{\text{tr}}, \mathbf{x}_2^{\text{tr}}, \dots, \mathbf{x}_{N_{\text{tr}}}^{\text{tr}}\}$ where N_{tr} is the number of videos in the training data and $\mathbf{x}_i^{\text{tr}} = (x_{i,1}^{\text{tr}}, \dots, x_{i,M}^{\text{tr}})$. $\mathbf{ADV}^{\text{tr}} = \{adv_1^{\text{tr}}, adv_2^{\text{tr}}, \dots, adv_{N_{\text{tr}}}^{\text{tr}}\}$. Similarly, validation data $\mathcal{X}^{\text{val}} = \{\mathbf{x}_1^{\text{val}}, \mathbf{x}_2^{\text{val}}, \dots, \mathbf{x}_{N_{\text{val}}}^{\text{val}}\}$ and $\mathbf{ADV}^{\text{val}} = \{adv_1^{\text{val}}, adv_2^{\text{val}}, \dots, adv_{N_{\text{val}}}^{\text{val}}\}$. A small constant ϵ (e.g., 0.1), $n_d = 5$. The number of synthetic samples N_{syn}.</p> <p>Output: model parameters and estimated total effects, dynamic total effects.</p> <p>Initialization: $\bar{L}^{\text{val}} = 0$, $\Delta L^{\text{val}} = 10$, initialize parameters θ_{GAN} and θ_{PiWAD}</p> <p># WGAN-GP layer learning</p> <p>while θ_{gen} not converge do</p> <p> for $i = 1, \dots, n_d$ do</p> <p> Generate random vectors \mathbf{z}; Generator samples $G_{\theta_{\text{gen}}}(\mathbf{z})$; Compute discriminator loss L_d according to Equation 9;</p> <p> Update discriminator weights $\theta_{\text{disc}} \leftarrow \text{Adam}(L_d, \theta_{\text{disc}})$.</p> <p> end for</p> <p> Compute generator loss L_g according to Equation 10.</p> <p> Update generator weights $\theta_{\text{gen}} \leftarrow \text{Adam}(L_g, \theta_{\text{gen}})$</p> <p>end while</p> <p>return generator weights θ_{gen}</p> <p># Generating synthetic samples</p> <p>Generate random vectors \mathbf{z}</p> <p>Generator samples $\tilde{\mathcal{X}} \leftarrow G_{\theta_{\text{gen}}}(\mathbf{z})$ where $\tilde{\mathcal{X}} = \{\tilde{\mathbf{x}}_1, \tilde{\mathbf{x}}_2, \dots, \tilde{\mathbf{x}}_{N_{\text{syn}}}\}$</p> <p># PiWAD learning</p> <p>while $\Delta L^{\text{val}} > \epsilon$ do</p> <p> for $i = 1, \dots, N_{\text{tr}}$ do</p> <p> Compute y_i^{pw} according to Equations 1 and 2; Compute y_i^{as} according to Equations 3-5; Compute y_i^{nh} according to Equations 6 and 7; Compute \widehat{adv}_i according to Equation 15.</p> <p> end for</p> <p> Compute MSE loss L^{tr} and update PiWAD model weights $\theta_{\text{PiWAD}} \leftarrow \text{Adam}(L^{\text{tr}}, \theta_{\text{PiWAD}})$</p> <p> for $i = 1, \dots, N_{\text{val}}$ do</p> <p> Compute y_i^{pw} according to Equations 1 and 2; Compute y_i^{as} according to Equations 3-5; Compute y_i^{nh} according to</p>
--

```

Equations 6 and 7; Compute  $\widehat{adv}_i$  according to Equation 15.
end for
Compute MSE loss in validation set  $L^{\text{val}}$ 
Compute MSE loss change in validation set:  $\Delta L^{\text{val}} = |L^{\text{val}} - \bar{L}^{\text{val}}|$ 
Update  $\bar{L}^{\text{val}} \leftarrow L^{\text{val}}$ 
end while
return  $\Theta_{\text{PiWAD}}$ 
# Effects estimation
for  $j = 1, \dots, M$  do
  for  $c$  in all possible  $X_j$  values:
    Compute dynamic total effect  $\Delta \widehat{ADV}(X_j = c)$  according to Equations 9-11.
    Compute total effect  $\Delta \widehat{ADV}(X_j)$  according to Equation 12.
  end for
return  $\Delta \widehat{ADV}(X_j), \forall j; \Delta \widehat{ADV}(X_j = c), \forall c, j$ 

```

Figure 1. The Algorithm of GAN-PiWAD

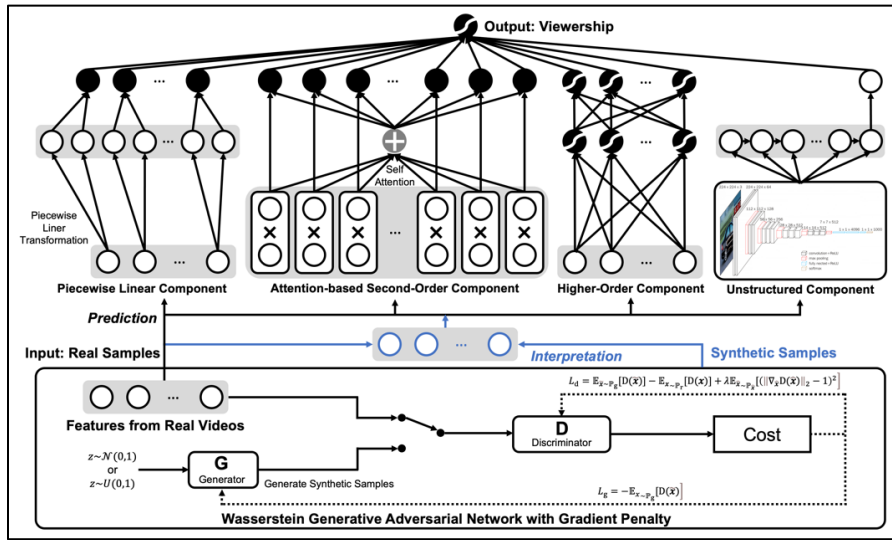


Figure 2. The Architecture of GAN-PiWAD

3.2.8. Novelty of GAN-PiWAD

Compared to the state-of-the-art deep learning methods in video analytics, GAN-PiWAD has five novelties: 1) In addition to maintaining the superior predictive power of deep learning, our method is also capable of disclosing the effect of each input feature on the output. 2) We extend the W&D framework by incorporating an unstructured component. This component is able to boost predictive performance for unstructured data analytics. 3) GAN-PiWAD incorporates the interaction effect among multi-modal inputs in the W&D framework. To avoid quadratic increase of parameters, we further devise an attention mechanism in the interaction component. 4) We design a fine-grained WGAN-GP component in W&D, so that our method is able to offer a precise estimation of the total effect. 5) In order to capture the dynamic total effect for each feature, our model predicts the total effect at every feature value. The

complex total effect when the feature varies can be modeled by our method.

4. Empirical Analyses

4.1. Study 1: YouTube Viewership Prediction

4.1.1. Data Preparation

Due to the societal impact and feature selection, we examine the utility of GAN-PiWAD in the healthcare context. We collected videos from the most well-known health organizations' YouTube channels, including NIH, CDC, WHO, FDA, Mayo Clinic, Harvard Medicine, Johns Hopkins Medicine, MD Anderson, and Jama Network. In addition, we collected the third-party YouTube videos that share the same keywords as listed in the above nine channel's playlists. In the end, we generated a dataset consisting of 6,528 videos and their webpages. The summary statistics are shown in Appendix 1.

Our features come from six sources: videos, audios, transcripts, video descriptions, webpages, and creators' channels. The raw videos are directly fed into our model via the unstructured component. We also generate the commonly adopted video features using the BRISQUE measurement (Mittal et al. 2012). In order to generate video features in a scalable and timely manner, we develop a python-based parallel processing method with 12 CPUs, which significantly reduced the expected computational time from 39 days to 7 days. To generate acoustic features, we separate the audio tracks from the videos. We utilize the Liborosa method to compute the acoustic features (Mcfee et al. 2015). In order to generate transcripts from audios, we develop a speech recognition model based on DeepSpeech (Hannun et al. 2014). This speech recognition model is trained on American English with synthetic noise augmentation that achieves a 7.06% word error rate on the LibriSpeech corpus (Panayotov et al. 2015). The trained speech recognition model is able to translate audios into transcripts. The description, webpage, and channel features are extracted directly from the webpage HTML files. A description of all the features and the methods to generate them are available in Appendix 2. In total, we generated 854 features.

4.1.2. Evaluation of Predictive Performance

We first evaluate the prediction performance of our method and the baselines. We then perform ablation studies. Lastly, we evaluate the interpretability of our method. We design three groups of baselines:

conventional ML (Abbasi and Chen 2008; Arazy et al. 2016; Zhang et al. 2016), deep learning methods (Xie et al. 2017, Xie and Zhang 2018), and interpretable methods (Cheng et al. 2016, Guo et al. 2020, Lee and Chan 2019, Tosun et al. 2020, Ye et al. 2019). The baseline models are detailed in Appendix 3. We adopt four common evaluation metrics: mean squared error (MSE), mean absolute error (MAE), mean squared logarithmic error (MSLE), and mean absolute logarithmic error (MALE). The calculation of these metrics is shown in Appendix 4. For all the following analyses, we adopt 10-fold cross validation where the dataset is divided into 10 folds. Each time we use one fold (10%) for test, one fold (10%) for validation, and eight folds (80%) for training. All the performances in the empirical analysis are the average performance of 10 times for each model. Table 2 shows the comparison with conventional ML.

Table 2. Comparison of GAN-PiWAD with Conventional Machine Learning

Method	MSE	MAE	MSLE	MALE
GAN-PiWAD (Ours)	165.442	6.244	0.992	0.813
Linear regression	285.585***	8.312***	2.924***	0.944**
KNN-1	196.114***	7.827***	2.961***	0.899**
KNN-3	183.257***	7.738***	2.994***	0.923**
KNN-5	398.577***	10.835***	4.294***	1.093***
DT-MSE	382.407***	10.256***	3.624***	0.998***
DT-MAE	374.503***	9.981***	4.065***	1.035***
DT-Fredmanmse	216.523***	6.646*	2.701***	0.902**
SVR-Linear	185.616***	9.567***	4.726***	1.259***
SVR-RBF	219.136***	6.765*	2.836***	0.899**
SVR-Poly	201.043***	7.609**	3.658***	1.035***
SVR-Sigmoid	398.577***	10.835***	4.294***	1.093***
Gaussian Process-1	999.376***	19.434***	20.619***	1.403***
Gaussian Process-3	999.376***	19.434***	20.619***	1.403***
Gaussian Process-5	999.376***	19.434***	20.619***	1.403***

*: $p < 0.05$; **: $p < 0.01$; ***: $p < 0.001$

GAN-PiWAD outperforms all baselines in all metrics. Compared with the best ML method KNN-3, GAN-PiWAD reduces MSE by 17.815 ($p < 0.001$). Even though KNN achieves relatively decent performance among the baselines, it is model-free that does not provide feature-based interpretation.

We, then, compare GAN-PiWAD with deep learning methods in Table 3. Compared with the best deep learning method LSTM-2, GAN-PiWAD reduces MSE by 26.467 ($p < 0.001$). GAN-PiWAD remains the best when the hidden layers of the baseline models change.

Table 3. Comparison of GAN-PiWAD with Deep Learning Methods

Method-Layer	MSE	MAE	MSLE	MALE
GAN-PiWAD (Ours)	165.442	6.244	0.992	0.813
MLP-1	364.064***	14.954***	3.094***	1.511***
MLP-2	351.437***	14.075***	2.852***	1.433***
MLP-3	281.090***	7.978***	2.728***	1.273***
MLP-4	279.648***	7.892***	2.550***	1.213***

CNN-1	207.271***	8.452***	1.453***	1.013***
CNN-2	193.240***	8.032***	1.333***	0.971***
CNN-3	199.997***	8.355***	1.414***	1.005***
CNN-4	196.158***	8.010***	1.326***	0.970***
LSTM-1	271.600***	9.760***	1.692***	1.039***
LSTM-2	191.909***	7.626***	1.185***	0.898*
BLSTM-1	354.760***	11.046***	1.942***	1.087***
BLSTM-2	196.247***	7.789***	1.212***	0.913*

*: $p < 0.05$; **: $p < 0.01$; ***: $p < 0.001$; The number after the model indicates the number of hidden layers.

We also compare GAN-PiWAD with the state-of-the-art interpretable methods in Table 4. Compared with the best interpretable method W&D, GAN-PiWAD reduces MSE by 35.072 ($p < 0.001$).

Table 4. Comparison of GAN-PiWAD with Interpretable Deep Learning

Method	MSE	MAE	MSLE	MALE
GAN-PiWAD (Ours)	165.442	6.244	0.992	0.813
W&D (Cheng et al. 2016)	200.514***	7.717***	1.300***	0.972***
W&D-CNN (Lee and Chan 2019)	222.786***	7.869***	1.373***	1.060***
W&D-LSTM (Tosun et al. 2020)	217.988***	7.770***	1.343***	1.016***
W&D-BLSTM (Ye et al. 2019)	208.775***	7.727***	1.233***	0.978***
Piecewise W&D-10 (Guo et al. 2020)	268.205***	9.148***	1.696***	1.251***
Piecewise W&D-20 (Guo et al. 2020)	231.900***	7.978***	1.390***	1.225***

*: $p < 0.05$; **: $p < 0.01$; ***: $p < 0.001$; Piecewise W&D- i : divide the input into i intervals

We fine-tune the hyperparameters of GAN-PiWAD to search for the best predictive performance. The hyperparameters include the number of hidden layers and the number of neurons in each layer. We replace the higher-order component in GAN-PiWAD with other deep neural networks, including CNN, LSTM, and BLSTM, to evaluate the design choice. The fine-tuning results are shown in Appendix 5. The final model has 3 dense layers in the higher-order component and 16 neurons in each layer. To ensure fair comparison, all the baseline methods in Tables 2-4 underwent the same parameter tuning process. The results in Tables 2-4 are the final fine-tuned results.

We further perform ablation studies to test the efficacy of the individual components of GAN-PiWAD. Table 5 shows that removing any component of GAN-PiWAD negatively impacts the performance, suggesting optimal design choices.

Table 5. Ablation Studies

Method	MSE	MAE	MSLE	MALE
GAN-PiWAD	165.442	6.244	0.992	0.813
GAN-PiWAD without unstructured component	181.056**	6.725*	1.060*	0.936**
GAN-PiWAD without piecewise linear component	213.434***	7.759***	1.340***	1.094***
GAN-PiWAD without second-order component	187.401***	7.150***	1.107**	0.967***
GAN-PiWAD without high-order component	191.891***	7.205***	1.152**	0.984***
GAN-PiWAD with simple linear encoding	189.712***	6.256	1.063*	0.819
GAN-PiWAD with 10 ordinal one hot encoding	190.224***	6.299	1.047*	0.817
GAN-PiWAD with 20 ordinal one hot encoding	186.767**	6.281	0.994	0.820
GAN-PiWAD with 10 ordinal encoding	191.969***	6.302	1.149***	0.833
GAN-PiWAD with 20 ordinal encoding	195.750***	6.383	1.319***	0.887*

GAN-PiWAD without attention	175.104*	6.626	1.053*	0.883*
-----------------------------	----------	-------	--------	--------

*: $p < 0.05$; **: $p < 0.01$; ***: $p < 0.001$

In order to test the effectiveness of each feature group, we remove each feature group stepwise and test its contribution to the performance. Appendix 6 shows the ablation analysis on feature groups by data source. The results show that removing any feature group will hamper the performance.

4.1.3. Interpretation of GAN-PiWAD

GAN-PiWAD offers precise total effect using Equations 8-12 because the WGAN-GP layer could generate samples to approximate the data distribution. The training results of the generative process are reported in Appendix 7. We perform ablation studies to test alternative generative models, including VAE and Bayesian Network, reported in Table 6. We first use Principle Component Analysis to reduce the feature dimension, which resulted in 10 major dimensions. Table 6 suggests only WGAN-GP can generate samples that have statistically no difference from the real samples in means and variances. We plot the feature-based interpretations in Figure 3¹. The original values are in Appendix 8. The interpretation indicates association, not causation.

Table 6. Comparison of WGAN-GP, VAE, and Bayesian Network

	Comp 1	Comp 2	Comp 3	Comp 4	Comp 5	Comp 6	Comp 7	Comp 8	Comp 9	Comp 10
Mean Comparison (p-value is the significance of t-tests comparing each model to the real samples)										
Real	-2.091	0.434	0.007	-0.104	-0.157	-0.257	0.031	0.032	-0.194	-0.039
WGAN-GP	-2.073	0.592	0.177	-0.295	-0.317	-0.172	0.018	0.051	-0.057	-0.031
P-value	0.859	0.238	0.204	0.059	0.062	0.277	0.863	0.793	0.035	0.919
VAE	2.068	-0.370	-0.410	0.296	0.190	0.243	-0.013	0.003	0.153	0.045
P-value	0.000	0.019	0.088	0.100	0.095	0.020	0.785	0.865	0.024	0.591
Bayesian	2.096	-0.656	0.226	0.103	0.284	0.185	-0.036	-0.086	0.097	0.025
P-value	0.000	0.000	0.428	0.371	0.024	0.008	0.723	0.508	0.100	0.685
Variance Comparison (p-value is the significance of F-tests comparing each model to the real samples)										
Real	0.528	0.751	0.837	0.551	0.474	0.423	0.403	0.476	0.347	0.323
WGAN-GP	0.706	0.795	0.707	0.531	0.457	0.509	0.503	0.447	0.473	0.335
P-value	0.302	0.613	0.951	0.093	0.746	0.924	0.417	0.437	0.274	0.768
VAE	1.825	2.509	1.619	1.845	1.476	1.526	1.370	1.293	1.161	0.876
P-value	0.000	0.004	0.080	0.175	0.018	0.014	0.401	0.721	0.653	0.005
Bayesian	2.067	2.321	2.328	1.644	1.724	1.479	1.441	1.312	1.367	1.436
P-value	0.000	0.000	0.971	0.685	0.009	0.023	0.402	0.762	0.696	0.527

The transcript and description features have a salient influence on the prediction. The transcript directly reflects the video content, and the description is a paragraph summarizing the content. These features include the number of medical terms, informativeness, readability, and complexity. The results

¹ For visualization simplicity, we average over all the video features into one feature, as they all represent the video quality with the same scale. We also average over all the acoustic features into one feature, because they measure the audio quality with the same scale. In order to compare all the features in the same scale, we normalized the effect values.

show that one unit of increase in transcript readability results in an increase of 757.402 average daily views. Medical knowledge, operationalized as the number of medical terms, has a sizable influence on the prediction as well. One unit of increase in the transcript medical terms will raise the average daily views by 440.649. These features measure how well the video can be perceived and how much medical information it contains. An easy-to-read and medically informative transcript or description leads to better engagement as the viewers attempt to seek medical information from the videos. Conveying the medical information that the viewers wanted to the largest extent could entertain the viewers and retain them to watch the rest of the video. If the medical information is easy to comprehend, the viewers have a better understanding of the video topic, which motivates them to watch the details from the video.

The transcript and description sentiments also significantly affect the prediction. A unit of increase in the transcript or description sentiment scores leads to an increase of 0.146-0.784 units in average daily views. These sentiments in the video bring in personal opinions and experience, which are relatable to viewers, thus enticing stronger viewer engagement.

The channel features have a critical influence on the prediction as well. In particular, if a channel is verified, the average daily views increase by 0.443 units. YouTube collects information from verified channels, such as phone numbers. Verified channels signal authenticity and credibility to viewers. Therefore, the viewers are more likely to watch the videos posted by these channels.

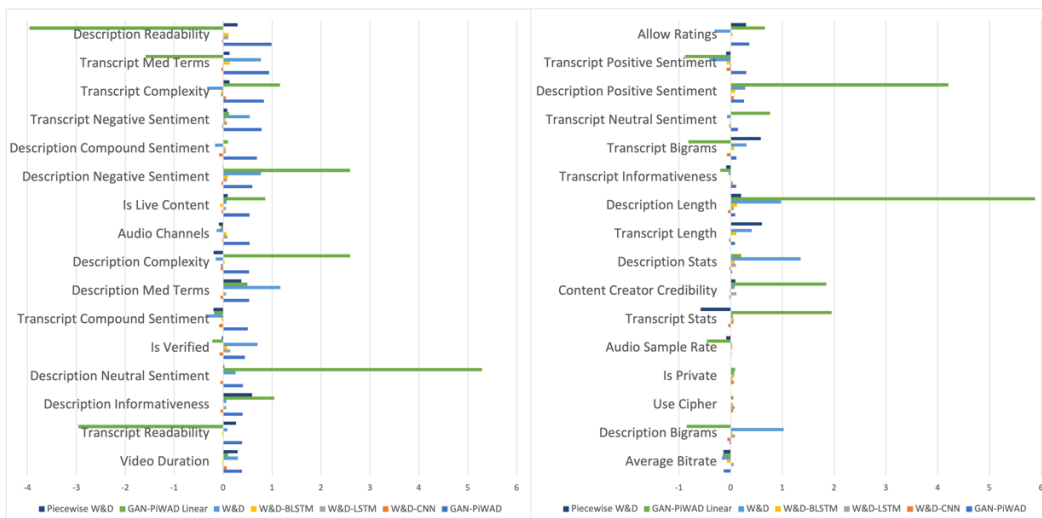


Figure 3. Feature-based Interpretation (Normalized, Study 1)

Our proposed method corrected the estimation error, while the existing methods could only offer the approximated estimation using the main effect. The error correction of our method has significant improvement on the model interpretation. For instance, our method interprets description readability to have a positive influence on video engagement. This is because readable descriptions are easy to comprehend, thus attracting viewers. However, the baseline models interpret description readability to have a negative influence, contradicting common sense. We also quantify the influence of the interpretation error correction in Table 7. We bolded the ones where the total effect and the main effect have an opposite direction.

Table 7. Interpretation Error Correction (Normalized, Study 1)

Feature	Total Effect	Main Effect	Feature	Total Effect	Main Effect
Use Cipher	0.000	0.053	Description Compound Sentiment	0.690	0.099
Is Private	0.000	0.086	Description Med Terms	0.530	0.496
Is Live Content	0.539	0.858	Transcript Bigrams	0.109	-0.816
Video Duration	0.384	0.100	Transcript Length	0.084	0.009
Average Bitrate	-0.135	-0.151	Transcript Complexity	0.834	1.160
Audio Sample Rate	0.000	-0.459	Transcript Readability	0.390	-2.959
Audio Channels	0.539	-0.053	Transcript Informativeness	0.105	-0.200
Description Bigrams	-0.020	-0.853	Transcript Stats	0.000	1.952
Description Length	0.086	5.882	Transcript Negative Sentiment	0.784	0.120
Description Complexity	0.533	2.594	Transcript Neutral Sentiment	0.140	0.759
Description Readability	0.989	-3.959	Transcript Positive Sentiment	0.301	-0.882
Description Informativeness	0.396	1.043	Transcript Compound Sentiment	0.503	-0.186
Description Stats	0.025	0.200	Transcript Med Terms	0.940	-1.588
Description Negative Sentiment	0.595	2.594	Content Creator Credibility	0.000	1.852
Description Neutral Sentiment	0.400	5.288	Is Verified	0.443	-0.221
Description Positive Sentiment	0.259	4.209			

Figure 3 shows the average total effect of each feature. GAN-PiWAD is also capable of estimating the dynamic total effect. Below, we randomly select three features and show how our method captures the dynamic total effect (Description complexity, description readability, and transcript negative sentiment). Figure 4.a. shows that the total effect of description complexity is positive when description complexity is low. Such a total effect turns negative when description complexity is high. This is because when description complexity is low, increasing complexity makes the description more formal and authoritative. Viewers watch it more because they trust it. As the complexity continues to increase, the description becomes too hard to comprehend and viewers lose interest in the video. Figure 4.b. shows that the total effect of description readability increases when the readability value increases. This could be because when the description is readable, it is also easier for the viewers to understand the medical knowledge and other content in the video. Figure 4.c. indicates that the total effect of transcript negative

sentiment increases when the value of transcript negative sentiment increases. When a video is enriched with negative sentiment, it usually contains opinions and commentaries, which may be relatable to the viewer’s personal experience or belief and even entice the viewers to write comments. Those interactions in the comment section further enhance video engagement.

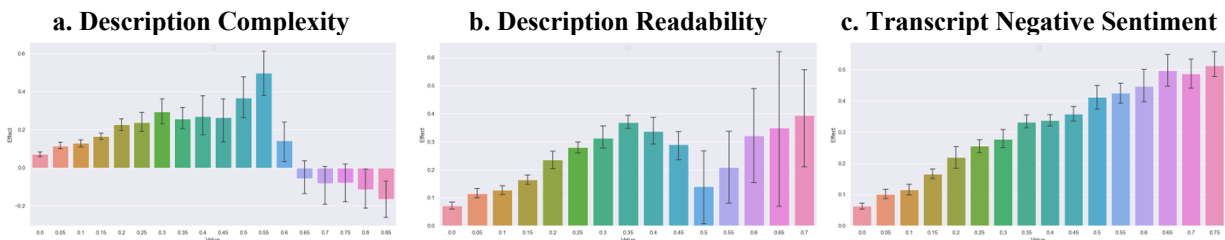


Figure 4. Examples of the Dynamic Total Effect (Study 1)

4.2. Study 2: Second Dataset for Robustness – Misinformation Videos

Among all the YouTube videos, health misinformation is the most concerning, as it leads viewers to institute ineffective, unsafe, costly, or inappropriate protective measures; undermine public trust in evidence-based health messages and interventions; and lead to a range of collateral negative consequences (Schillinger et al. 2020). During a pandemic, widespread health misinformation jeopardizes the efforts of already-challenging disease control and prevention. For instance, a popular myth during the COVID-19 pandemic – that highly concentrated alcohol consumption could disinfect the body – claimed over 800 lives and caused more than 5,800 hospitalizations (Islam et al. 2020). Successful containment of misinformation hinges on accurate prediction of misinformation spread as well as the understanding of the factors. Study 2 evaluates GAN-PiWAD by predicting health misinformation video viewership.

A number of trusted news outlets have identified a set of videos with health misinformation on YouTube. The factchecking links of these videos are shown in Appendix 10. We crawled all the videos reported by these sources, including 4,445 misinformation videos and their webpages. Table 8 reports the comparison with all the baseline models.

Table 8. Comparison of GAN-PiWAD with Baseline Models (Study 2)

Method	MSE	MAE	MSLE	MALE	Method	MSE	MAE	MSLE	MALE
GAN-PiWAD (Ours)	140.202	4.865	0.728	0.642	MLP-3	162.249**	6.305***	0.950**	0.817***
Linear regression	881.027***	12.812***	3.184***	0.891***	MLP-4	181.192***	6.128**	0.932**	0.854***
KNN-1	227.479***	6.944***	2.421***	0.748**	CNN-1	245.382***	7.987***	1.377***	0.932***
KNN-3	163.061**	6.487***	2.327***	0.757**	CNN-2	158.040**	6.741***	1.090***	0.862***
KNN-5	180.479***	6.309***	2.264***	0.758**	CNN-3	155.651*	6.481***	1.023***	0.832***
DT-MSE	284.387***	8.433***	3.362***	0.901***	CNN-4	169.584**	6.633***	1.065***	0.849***

DT-MAE	288.223***	8.439***	3.193***	0.870***	LSTM-1	341.301***	9.715***	1.718***	0.973***
DT-Fredmannse	299.519***	8.725***	3.435***	0.919***	LSTM-2	182.828***	6.955***	1.099***	0.846***
SVR-Linear	185.644***	9.483***	4.924***	1.267***	BLSTM-1	367.261***	9.728***	1.661***	0.973***
SVR-RBF	185.989***	9.455***	4.901***	1.263***	BLSTM-2	175.995***	6.645***	0.999***	0.801***
SVR-Poly	192.951***	9.576***	4.910***	1.267***	W&D (Cheng et al. 2016)	180.869***	6.015**	1.067**	0.819**
SVR-Sigmoid	185.646***	9.483***	4.924***	1.267***	W&D-CNN (Lee and Chan 2019)	186.773***	6.304**	1.866**	1.039***
Gaussian Process-1	1291.331***	23.791***	8.508***	1.579***	W&D-LSTM (Tosun et al. 2020)	183.719***	6.141**	1.598***	0.943***
Gaussian Process-3	1291.331***	23.791***	8.508***	1.579***	W&D-BLSTM (Ye et al. 2019)	206.321***	6.648**	2.454***	1.210***
Gaussian Process-5	1291.331***	23.791***	8.508***	1.579***	Piecewise W&D-10 (Guo et al. 2020)	227.633***	7.126***	3.116***	1.420***
MLP-1	172.460***	6.011**	1.005***	0.801***	Piecewise W&D-20 (Guo et al. 2020)	206.792***	6.805***	3.016***	1.395***
MLP-2	169.147***	6.561***	1.063***	0.847***					

*, $p < 0.05$; **, $p < 0.01$; ***, $p < 0.001$

GAN-PiWAD outperforms all the baseline methods in all four metrics. Compared to the best machine learning baseline model (KNN-3), GAN-PiWAD drops MSE by 11.398. Compared with the best deep learning method (CNN-3), GAN-PiWAD reduces MSE by 3.988. Compared with the best interpretable model (W&D), GAN-PiWAD reduces the MSE by 29.206.

Table 9 reports the ablation study results. Excluding any component negatively impacts the performance, suggesting each component has a significant contribution to the overall performance.

Table 9. Ablation Studies in Study 2

Method	MSE	MAE	MSLE	MALE
GAN-PiWAD	140.202	4.865	0.728	0.642
GAN-PiWAD without unstructured component	151.259*	5.369	0.887*	0.712*
GAN-PiWAD without piecewise linear component	175.136**	5.717*	0.915*	0.766*
GAN-PiWAD without second-order component	155.984*	5.298	0.890*	0.773*
GAN-PiWAD without high-order component	159.354*	5.338	0.848	0.707*
GAN-PiWAD with simple linear encoding	153.454*	5.288	0.872**	0.725*
GAN-PiWAD with 10 ordinal one-hot encoding	167.449**	5.412	0.938**	0.758*
GAN-PiWAD with 20 ordinal one-hot encoding	168.621**	5.355	0.968***	0.736*
GAN-PiWAD with 10 ordinal encoding	195.510***	6.427***	2.862***	1.374***
GAN-PiWAD with 20 ordinal encoding	195.510***	6.427***	2.862***	1.374***
GAN-PiWAD without attention	153.454*	5.288	0.872**	0.688*

*, $p < 0.05$; **, $p < 0.01$; ***, $p < 0.001$

Similar to Study 1, we perform all the other empirical analyses for Study 2, including summary statistics, hyperparameter tuning, ablation analysis in feature group, training results of the generative process, and the ablation comparison with Bayesian Network and VAE. These results are reported in Appendix 9. The conclusions are consistent with Study 1 and in favor of our method.

We also interpret the prediction of Study 2 in Figure 5. The feature effect original values, interpretation error correction, and dynamic total effects are reported in Appendix 11. The interpretation indicates that the textual features and sentiments of transcript and description are critical features associated with misinformation video popularity. The interpretation of the prediction sheds light on the management of video credibility for video sharing platforms. These platforms could utilize our method to

monitor the transcript and description features. Medical-related videos whose description is well perceived should be under scrutiny. When a video shows overwhelmingly negative content, it needs to be closely monitored as well to prevent misinformation spread widely.

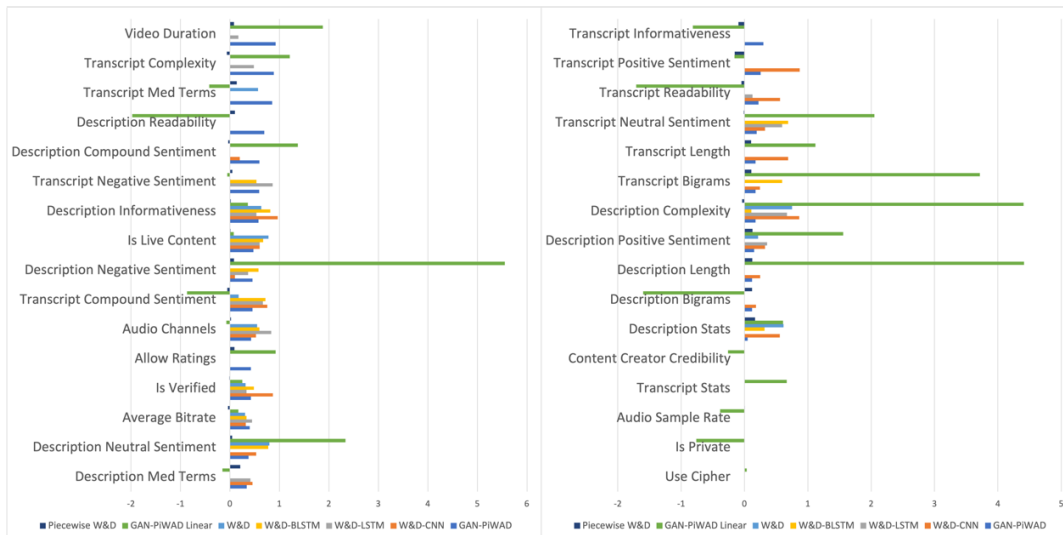


Figure 5. Feature-based Interpretation (Normalized, Study 2)

4.3. Evaluation of Interpretability

To quantify the interpretability of our method and the baseline methods, we design a user study. We devise five groups: GAN-PiWAD, W&D, piecewise W&D, SHAP, and VAE (replace GAN with VAE in our model). The rationale for choosing these models is articulated in Appendix 12. We recruited 174 students from two national universities in Asia. They were randomly assigned to one of the five groups. To ensure randomization, we selected nine control variables: age, gender, education, knowledge in computer science, knowledge in ML, video watching frequency, video uploading experience, trust in AI and automation, and health literacy. The summary statistics of the control variables are shown in Appendix 14. We perform one-way ANOVA on the control variables and the outcome variable (interpretability) for randomization checks. The result, reported in Appendix 15, indicates the control variables do not affect interpretability. The full survey can be found in Appendix 13.

The participants were notified they would be assigned a ML model to predict the daily viewership of a YouTube video. We would show them the variables the model uses and the weights of the variables. We disclosed that the more reasonable these variables and weights are, the more accurate the prediction

would be, and that their compensation is positively related to the prediction performance.

To ensure the participants understand what the variables and weights mean, we designed a training session. We displayed a pseudo model, shown in Figure 6. We informed them the weight of a variable indicates the importance of the variable. We showed one example: “If the weight of a variable is 0.3, this means increasing this variable by 1 unit, the model’s prediction of this video's daily viewership will increase by 0.3 units.” After that, we designed two test questions to teach them how to read the model:

1. **Question:** According to the above figure, when using the above model to predict the daily viewership of videos, what are the top two essential variables that have positive effects?
Options: Variable 1, Variable 2, Variable 3, Variable 4, Variable 5, Variable 6, Variable 7
2. **Question:** According to the weights in the figure, if variable 6 increases by 1 unit, how will the above model prediction of video viewership change?
Options: Increase by 0.3 unit, Increase by 0.6 unit, Decrease by 0.3 unit, Decrease by 0.6 unit

If the participants choose an incorrect answer, an error message and a hint will appear on the screen, shown in Appendix 16. They need to find the correct answer before proceeding to the next page.

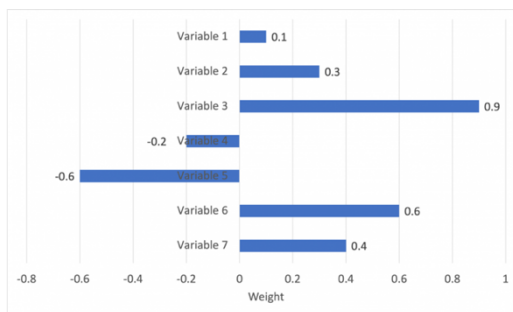


Figure 6. Pseudo Model in the Training Session

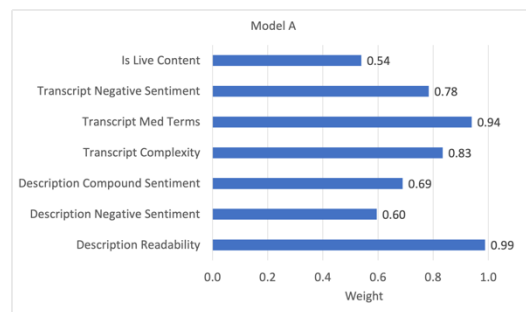


Figure 7. Model Displayed in the User Study

In the experiment, we first ask the participants to watch a YouTube video to familiarize the prediction target and context. We then show them a screenshot of the video webpage (Appendix 17), depicting the potential variables we can use for prediction. Then, we show them the variables and weights of their model (Figure 7). We choose the seven most important variables by weight, because seven is considered the “Magical Number” in psychology and is the limit of our capacity to process short-term information (Miller 1956). To help the participants fully understand Figure 7, we design four test questions:

1. **Question:** According to the above figure, when using the above model to predict video viewership, please rank the following variables from the most important to the least important used by the model. Please put the most important variable on the top and the least important on the bottom. You can drag the variables to reorder. Hint: The importance of a variable in a prediction can be measured by the weight of the variable.
Options: The seven variables in a randomized order
2. **Question:** What are the top 2 most essential variables in the above model?

- Options:** Description readability, Description negative sentiment, Transcript med terms, Transcript complexity
3. **Question:** If the creator of the above video would like to increase video viewership, which of the following option is more effective?
Options: Increase "Is live content" by 1 unit, Increase "Transcript negative sentiment" by 1 unit
4. **Question:** According to the weights in the figure, if the "Description negative sentiment" increases by 1 unit, how will the above model prediction of video viewership change?
Options: Increase by 1 unit, Increase by 0.6 unit, Decrease by 1 unit, Decrease by 0.6 unit

If the participants choose an incorrect answer, an error message and a hint will appear on the screen, shown in Appendix 18. They need to find the correct answer before proceeding to the next page.

After answering the previous questions correctly, the participants have a good understanding of the model. We then ask them to rate the interpretability of the model. The literature review suggests that “interpretability is related to how well humans trust some information by looking and reasoning about it.” We adopt trust in automated systems as the first interpretability measurement (Chai et al. 2014, Jian et al. 2010). Dhurandhar et al. (2017) suggests “AI is interpretable to the extent that the produced interpretation is able to maximize a user’s target performance.” Our target is viewership prediction. Following Dhurandhar’s definition and similar designs in Lee et al. (2018), models that are more useful for viewership prediction decision is more interpretable. We adopt usefulness as the second interpretability measurement. The two measurement scales can be found in Appendix 13. The Cronbach’s Alpha is 0.963 for the trust in automated systems scale in our study, and 0.975 for the usefulness scale, suggesting excellent reliability. The factor loadings are shown in Appendix 19, showing great validity. We perform *t*-tests in Table 10 on our method and the other four groups to compare interpretability. We designed an attention check question in the scales (“Please just select neither agree or disagree”). After removing those who failed the attention check, we have 152 remaining participants.

Table 10: Comparison of Interpretability for GAN-PiWAD and Other Interpretable Methods

Group	Mean of Interpretability: Trust	<i>P</i> -value of T-test with GAN-PiWAD	Mean of Interpretability: Usefulness	<i>P</i> -value of T-test with GAN-PiWAD
GAN-PiWAD	2.415	NA	2.433	NA
W&D	1.559	2.83E-05***	1.500	6.40E-06***
Piecewise W&D	0.606	1.06E-14***	0.495	3.83E-15***
SHAP	1.378	4.20E-06***	1.255	5.77E-07***
VAE	1.202	3.60E-06***	1.160	3.10E-06***

GAN-PiWAD has significant better interpretability than other methods. Compared with the best alternative method W&D, GAN-PiWAD improves the user-rated interpretability by 55% (trust

measurement) and 62% (usefulness measurement). Such improvement is attributed to GAN-PiWAD’s ability to compute the precise total effect.

The above analysis shows the between-group comparison of different models. We further investigate which model each participant would finally adopt. We tell the participants that they have a chance to decide whether to keep the current model. If they think the variables and weights of the previous model are not reasonable, they have a chance to change to a different model. To motivate them to choose the most reasonable model, we inform them that their compensation is positively related to the prediction performance. Then we show them the variables and weights of all the five models, similar to Figure 7. The order of the five models is randomized. We ask which model they would like to finally adopt for the prediction, and the trust in automated systems and usefulness scales are displayed again to measure the interpretability of the adopted model. The results are reported in Tables 11 and 12.

Table 11. Number of Participants in Each Original Model and Final Adopted Model

	Original: GAN-PiWAD	Original: Baseline
Switch to GAN-PiWAD	23	92
Switch to Baseline	7	30

Table 12. Comparison of 1st Time and 2nd Time Interpretability

	Mean of 1st Interpretability: Trust	Mean of 2nd Interpretability: Trust	T-test for Two Times	Mean of 1st Interpretability: Usefulness	Mean of 2nd Interpretability: Usefulness	T-test for Two Times
GAN-PiWAD → GAN-PiWAD	2.700	3.324	0.0001***	2.717	3.348	0.00049***
Baseline → GAN-PiWAD	0.924	2.616	2.20E-16***	0.868	2.583	< 2.2e-16***

115 participants (75.66%) finally adopted our model regardless of what model they were originally assigned. Table 12 shows for those who finally adopted our model, the 2nd time interpretability is higher than the 1st time. This is because after the participants see the five models, the relative advantage of our model is even more obvious, causing them to rate the interpretability of our model higher the second time.

5. Discussion

5.1. Implications to Information Systems

In line with the design science research guidelines (Hevner et al. 2004), this study identifies an impactful social media analytics problem: video engagement prediction. We demonstrate that no adequate solutions exist in the prior literature and develop a novel information system that predicts video engagement while interpreting prediction factors. We conduct comprehensive evaluations and interpretations of the

information system and design a user study to assess its utility. This study also fits in the computational genre of design science research (Rai 2017). The computational design science paradigm emphasizes an “interdisciplinary approach in developing novel data representations, computational algorithms, business intelligence, and analytics methods” (Rai 2017). Our study develops an interdisciplinary approach that involves a novel computational algorithm and an analytical solution to a major social problem, thus holding great potential for generating IS research with significant societal impact (Abbasi et al. 2018, Karahanna et al. 2018, Kitchens et al. 2018, Zhang et al. 2016b).

5.2. Methodological Implications

We devise a novel GAN-PiWAD method to predict video engagement and provide model interpretation. GAN-PiWAD innovatively models unstructured data, incorporates the interaction effect, estimates total effect more precisely, and captures the dynamic total effect. The new framework learns four components jointly (piecewise linear, attention-based interaction, higher-order, and unstructured). The prediction performance of GAN-PiWAD surpasses strong baselines. In order to tease out the influence from the high-order component, we introduce a WGAN-GP within the W&D framework. A user study confirms this approach significantly improves interpretability. Our feature interpretation enhances decisions and actions via improved trust and model usefulness. GAN-PiWAD is not restricted to the video engagement prediction context. It can be generalized to understand the underlying factors of other human behaviors, including healthcare, cybersecurity, and technology acceptance, among others.

5.3. Practical Implications

This study offers many practical implications for the stakeholders. For the video-sharing platforms, our method is an implementable analytics tool that can predict video viewership. Our method also offers the interpretation of this prediction. Since YouTube relies on the percentage of total views to manage video credibility, our method provides YouTube insights to design intervention measures to promote legitimate videos’ viewership and curb violative videos’ viewership. For instance, negative videos from verified channels with easy-to-read descriptions need to be specially monitored for misinformation. Content creators could leverage our method to predict their viewership in order to decide where to allocate more

budgets. Our interpretation also gives content creators directions to improve video engagement.

5.4. Limitations and Future Directions

This study has several limitations and areas for improvement. First, besides predicting video engagement, our method could also understand other human behaviors in healthcare, cybersecurity, and technology acceptance. However, new data types and representations need to be engineered to feed into the model. Future work could extend our method (data types, features, among others) to test its efficacy in other research contexts. Second, we focused our empirical analyses on YouTube videos. Other social media platforms, such as Facebook and Twitter, are also popular outlets for user engagement. More ground truth data could be collected from Facebook and Twitter to perform the empirical analyses.

6. Conclusion

Understanding video engagement is fundamental for content creators and video-sharing sites. This study proposes GAN-PiWAD for video engagement prediction and interpretation. To address the pitfalls of prior interpretable methods, our study incorporates an unstructured component, considers the feature interactions, and creates an innovative approach to estimate the precise total effect of as well as its dynamic changes. Empirical results indicate that GAN-PiWAD outperforms strong baseline models. This method holds the potential to be generalized to understand other human behaviors. A user study confirms that the interpretability of GAN-PiWAD is significantly better than other interpretable methods, particularly in improving trust and model usefulness. These findings offer implementable action plans for content creators and video sharing platforms to improve video engagement and manage video credibility.

References

- Abbasi A, Albrecht C, Vance A, Hansen J (2012) Metafraud: a meta-learning framework for detecting financial fraud. *MIS Quarterly* 36(4):1293–1327.
- Abbasi A, Chen H (2008) CyberGate: a design framework and system for text analysis of computer-mediated communication. *MIS Quarterly* 32(4):811–837.
- Abbasi A, Zhang Z, Zimbra D, Chen H, Nunamaker JF (2010) Detecting fake websites: the contribution of statistical learning theory. *MIS Quarterly* 34(3):435–461.
- Abbasi A, Zhou Y, Deng S, Zhang P (2018) Text analytics to support sense-making in social media: A language-action perspective. *MIS Quarterly* 42(2):427–464.
- Agarwal R, Frosst N, Zhang X, Caruana R, Hinton GE (2020) Neural Additive Models: Interpretable Machine Learning with Neural Nets.
- Alqahtani H, Kavakli-Thorne M, Gulshan Kumar · (2021) Applications of Generative Adversarial Networks

- (GANs): An Updated Review. *Archives of Computational Methods in Engineering* 28:525–552.
- Arazy O, Daxenberger J, Lifshitz-Assaf H, Nov O, Gurevych I (2016) Turbulent Stability of Emergent Roles: The Dualistic Nature of Self-Organizing Knowledge Coproduction. *Information Systems Research* 27(4):792–812.
- Bach S, Binder A, Montavon G, Klauschen F, Müller KR, Samek W (2015) On Pixel-Wise Explanations for Non-Linear Classifier Decisions by Layer-Wise Relevance Propagation. *PLOS ONE* 10(7):e0130140.
- Breiman L (2001) Statistical Modeling: The Two Cultures. <https://doi.org/10.1214/ss/1009213726> 16(3):199–231.
- Burel G, Saif H, Alani H (2017) Semantic wide and deep learning for detecting crisis-information categories on social media. *Lecture Notes in Computer Science*. 138–155.
- Caruana R, Lou Y, Microsoft JG, Koch P, Sturm M, Elhadad N (2015) Intelligible Models for HealthCare: Predicting Pneumonia Risk and Hospital 30-day Readmission. *Proceedings of the 21th ACM SIGKDD International Conference on Knowledge Discovery and Data Mining*.
- Chai S, Das S, Rao HR (2014) Factors Affecting Bloggers' Knowledge Sharing: An Investigation Across Gender. <http://dx.doi.org/10.2753/MIS0742-1222280309> 28(3):309–342.
- Chen X, Duan Y, Houthoofd R, Schulman J, Sutskever I, Abbeel P (2016) InfoGAN: Interpretable Representation Learning by Information Maximizing Generative Adversarial Nets. *NIPS 2016*.
- Cheng HT, Koc L, Harmsen J, Shaked T, Chandra T, Aradhye H, Anderson G, et al. (2016) Wide & deep learning for recommender systems. *ACM International Conference Proceeding Series*. 7–10.
- Das A, Rad P (2020) Opportunities and Challenges in Explainable Artificial Intelligence (XAI): A Survey.
- Dayan P, Hinton GE, Neal RM, Zemel RS (1995) The Helmholtz Machine. *Neural Computation* 7(5):889–904.
- Dhurandhar A, Iyengar V, Luss R, Shanmugam K (2017) TIP: Typifying the Interpretability of Procedures.
- Dietvorst BJ, Simmons JP, Massey C (2015) Algorithm aversion: People erroneously avoid algorithms after seeing them err. *Journal of Experimental Psychology: General* 144(1):114–126.
- Doshi-Velez F, Kim B (2017) Towards A Rigorous Science of Interpretable Machine Learning.
- Fang X, Hu PJH, Li ZL, Tsai W (2013) Predicting adoption probabilities in social networks. *Information Systems Research* 24(1):128–145.
- Goodfellow I, Bengio J, Courville A (2016) *Deep Learning*
- Goodfellow IJ, Pouget-Abadie J, Mirza M, Xu B, Warde-Farley D, Ozair S, Courville AC, Bengio Y (2014) Generative Adversarial Nets. *NIPS 2014*.
- Goyal Y, Feder A, Shalit U, Kim B (2019) Explaining Classifiers with Causal Concept Effect (CaCE).
- Gulrajani I, Ahmed F, Arjovsky M, Dumoulin V, Courville A (2017) Improved Training of Wasserstein GANs. *Advances in Neural Information Processing Systems 30 (NIPS 2017)*. 5767–5777.
- Guo H, Tang R, Ye Y, Li Z, He X, Dong Z (2018) DeepFM: An End-to-End Wide & Deep Learning Framework for CTR Prediction.
- Guo M, Zhang Q, Liao X, Zeng DD (2020) An interpretable neural network model through piecewise linear approximation.
- Han Y, Chen W, Xiong X, Li Q, Qiu Z, Wang T (2019) Wide & Deep Learning for improving Named Entity Recognition via Text-Aware Named Entity Normalization. *Thirty-Third AAAI Conference on Artificial Intelligence 2019*.
- Hannun A, Case C, Casper J, Catanzaro B, Diamos G, Elsen E, Prenger R, et al. (2014) Deep Speech: Scaling up end-to-end speech recognition. *arXiv*.
- Heider F, Simmel M (1944) An Experimental Study of Apparent Behavior. *The American Journal of Psychology* 57(2):243.
- Hevner AR, March ST, Park J, Ram S (2004) Design Science in Information Systems Research. *MIS Quarterly* 28(1):75–105.
- Hinge Marketing (2021) What Is the Cost of Video Production for the Web? Retrieved (July 29, 2021), <https://hingemarketing.com/blog/story/what-is-the-cost-of-video-production-for-the-web>.
- Hoiles W, Aprem A, Krishnamurthy V (2017) Engagement and Popularity Dynamics of YouTube Videos and Sensitivity to Meta-Data. *IEEE Transactions on Knowledge and Data Engineering* 29(7):1426–1437.
- Hu Z, Yang Z, Liang X, Salakhutdinov R, Xing EP (2017) Toward Controlled Generation of Text. :1587–1596. (July 17) <http://proceedings.mlr.press/v70/hu17e.html>.

- Hubspot (2021) YouTube Marketing: The Ultimate Guide. Retrieved (August 19, 2021), <https://www.hubspot.com/youtube-marketing>.
- Islam MS, Sarkar T, Khan SH, Mostofa Kamal AH, Hasan SMM, Kabir A, Yeasmin D, et al. (2020) COVID-19–Related Infodemic and Its Impact on Public Health: A Global Social Media Analysis. *The American Journal of Tropical Medicine and Hygiene*:tpmd200812.
- Jian JY, Bisantz AM, Drury CG (2010) Foundations for an Empirically Determined Scale of Trust in Automated Systems. http://dx.doi.org/10.1207/S15327566IJCE0401_04 4(1):53–71.
- Jordan MI, Ghahramani Z, Jaakkola TS, Saul LK (1999) An Introduction to Variational Methods for Graphical Models. *Machine Learning 1999* 37:2 37(2):183–233.
- Karahanna E, Xu SX, Xu Y, Zhang N (2018) The needs-affordances-features perspective for the use of social media. *MIS Quarterly* 42(3):737–756.
- Kingma DP, Welling M (2013) Auto-Encoding Variational Bayes. *2nd International Conference on Learning Representations, ICLR 2014 - Conference Track Proceedings*.
- Kitchens B, Dobolyi D, Li J, Abbasi A (2018) Advanced Customer Analytics: Strategic Value Through Integration of Relationship-Oriented Big Data. *Journal of Management Information Systems* 35(2):540–574.
- Lee D, Manzoor E, Cheng Z (2018) Focused Concept Miner (FCM): Interpretable Deep Learning for Text Exploration. *SSRN Electronic Journal*.
- Lee JW, Chan YY (2019) Fine-Grained Plant Identification using wide and deep learning model. *2019 International Conference on Platform Technology and Service, PlatCon 2019 - Proceedings*.
- Linardatos P, Papastefanopoulos V, Kotsiantis S (2020) Explainable AI: A Review of Machine Learning Interpretability Methods. *Entropy 2021, Vol. 23, Page 18* 23(1):18.
- Liu X, Zhang B, Susarla A, Padman R (2020) Go to YouTube and Call Me in the Morning: Use of Social Media for Chronic Conditions. *MIS Quarterly*.
- Lundberg SM, Allen PG, Lee SI (2017) *A Unified Approach to Interpreting Model Predictions*
- Madathil KC, Rivera-Rodriguez AJ, Greenstein JS, Gramopadhye AK (2015) Healthcare information on YouTube: A systematic review. *Health Informatics Journal* 21(3):173–194.
- Mai F, Shan Z, Bai Q, Wang X (Shane), Chiang RHL (2018) How Does Social Media Impact Bitcoin Value? A Test of the Silent Majority Hypothesis. *Journal of Management Information Systems* 35(1):19–52.
- Mcfee B, Raffel C, Liang D, Ellis DPW, Mcvicar M, Battenberg E, Nieto O (2015) librosa: Audio and Music Signal Analysis in Python. *PROC. OF THE 14th PYTHON IN SCIENCE CONF*.
- Miller GA (1956) The magical number seven, plus or minus two: some limits on our capacity for processing information. *Psychological Review* 63(2):81–97.
- Miller T (2019) Explanation in artificial intelligence: Insights from the social sciences. *Artificial Intelligence* 267:1–38.
- Mittal A, Moorthy AK, Bovik AC (2012) No-reference image quality assessment in the spatial domain. *IEEE Transactions on Image Processing* 21(12):4695–4708.
- Molnar C (2019) *Interpretable Machine Learning*
- Montavon G, Binder A, Lapuschkin S, Samek W, Müller KR (2019) Layer-Wise Relevance Propagation: An Overview. *Lecture Notes in Computer Science (including subseries Lecture Notes in Artificial Intelligence and Lecture Notes in Bioinformatics)* 11700 LNCS:193–209.
- Murdoch WJ, Singh C, Kumbier K, Abbasi-Asl R, Yu B (2019) Definitions, methods, and applications in interpretable machine learning. *Proceedings of the National Academy of Sciences of the United States of America* 116(44):22071–22080.
- Neal RM (1992) Bayesian Mixture Modeling. *Maximum Entropy and Bayesian Methods*:197–211.
- NYTimes (2021) YouTube Discloses Percentage of Views That Go to Videos That Break its Rules - The New York Times. Retrieved (August 1, 2021), <https://www.nytimes.com/2021/04/06/technology/youtube-views.html>.
- Panayotov V, Chen G, Povey D, Khudanpur S (2015) Librispeech: An ASR corpus based on public domain audio books. *IEEE International Conference on Acoustics, Speech and Signal Processing - Proceedings*. 5206–5210.
- Rafique H, Wang T, Lin Q (2019) Model-Agnostic Linear Competitors -- When Interpretable Models Compete and Collaborate with Black-Box Models. *arXiv* 00(0):0–000.

- Rai A (2017) Editor's comments: diversity of Design Science Research. *MIS Quarterly* 41(1):iii–xviii.
- Ribeiro MT, Singh S, Guestrin C (2016) “Why should i trust you?” Explaining the predictions of any classifier. *Proceedings of the ACM SIGKDD International Conference on Knowledge Discovery and Data Mining* 13-17-August-2016:1135–1144.
- Richier C, Altman E, Elazouzi R, Altman T, Linares G, Portilla Y (2014) Modelling View-count Dynamics in YouTube.
- Saboo AR (2016) Using Big Data to Model Time-Varying Effects for Marketing Resource (RE) Allocation. *MIS Quarterly* 40(4):911–939.
- Schillinger D, Chittamuru D, Ramírez AS (2020) From “Infodemics” to Health Promotion: A Novel Framework for the Role of Social Media in Public Health. *American Journal of Public Health*:e1–e4.
- Selvaraju RR, Cogswell M, Das A, Vedantam R, Parikh D, Batra D (2017) Grad-CAM: Visual Explanations From Deep Networks via Gradient-Based Localization. :618–626. <http://gradcam.cloudev.org>.
- Stieglitz S, Dang-Xuan L (2013) Emotions and information diffusion in social media - Sentiment of microblogs and sharing behavior. *Journal of Management Information Systems* 29(4):217–248.
- Szabo G, Huberman BA (2010) Predicting the popularity of online content. *Communications of the ACM* 53(8):80–88.
- Tanner MA, Wong WH (1987) The calculation of posterior distributions by data augmentation. *Journal of the American Statistical Association* 82(398):528–540.
- Tosun N, Sert E, Ayaz E, Yilmaz E, Gol M (2020) Solar Power Generation Analysis and Forecasting Real-World Data Using LSTM and Autoregressive CNN. 1–6.
- Tsang M, Cheng D, Liu Y (2018) Detecting Statistical Interactions from Neural Network Weights. *6th International Conference on Learning Representations, ICLR 2018*.
- Varshney KR, Khanduri P, Sharma P, Zhang S, Varshney PK (2018) Why Interpretability in Machine Learning? An Answer Using Distributed Detection and Data Fusion Theory.
- Weller A (2017) Challenges for Transparency. *ICML*.
- WHO (2020) Managing the COVID-19 infodemic: Promoting healthy behaviours and mitigating the harm from misinformation and disinformation. Retrieved (September 28, 2020), <https://www.who.int/news-room/detail/23-09-2020-managing-the-covid-19-infodemic-promoting-healthy-behaviours-and-mitigating-the-harm-from-misinformation-and-disinformation>.
- Xie J, Liu X, Zeng D, Fang X (2017) Understanding Reasons for Medication Nonadherence: An Exploration in Social Media Using Sentiment-Enriched Deep Learning Approach. *ICIS 2017 Proceedings*.
- Xie J, Zhang B (2018) Readmission Risk Prediction for Patients with Heterogeneous Hazard: A Trajectory-Aware Deep Learning Approach. *ICIS 2018 Proceedings*.
- Ye H, Cao B, Peng Z, Chen T, Wen Y, Liu J (2019) Web Services Classification Based on Wide & Bi-LSTM Model. *IEEE Access* 7:43697–43706.
- Zeiler MD, Fergus R (2014) Visualizing and Understanding Convolutional Networks. *Lecture Notes in Computer Science (including subseries Lecture Notes in Artificial Intelligence and Lecture Notes in Bioinformatics)* 8689 LNCS(PART 1):818–833.
- Zhang D, Zhou L, Kehoe JL, Kilic IY (2016a) What Online Reviewer Behaviors Really Matter? Effects of Verbal and Nonverbal Behaviors on Detection of Fake Online Reviews. *Journal of Management Information Systems* 33(2):456–481.
- Zhang D, Zhou L, Kehoe JL, Kilic IY (2016b) What Online Reviewer Behaviors Really Matter? Effects of Verbal and Nonverbal Behaviors on Detection of Fake Online Reviews. *Journal of Management Information Systems* 33(2):456–481.
- Zhang X, Qian B, Cao S, Li Y, Chen H, Zheng Y, Davidson IN (2020) INPREM: An Interpretable and Trustworthy Predictive Model for Healthcare | Proceedings of the 26th ACM SIGKDD International Conference on Knowledge Discovery & Data Mining. *Proceedings of the 26th ACM SIGKDD International Conference on Knowledge Discovery & Data Mining*. 450–460.

Online Supplementary Materials

1. Summary Statistics of Study 1

Statistic	Min	Q ₁	Median	Mean	Q ₃	Max
View count	7	959	2681	9414.681	7126.5	305715
Allow ratings	0	1	1	0.977202	1	1
Is live content	0	0	0	0.100222	0	1
Published days	8	669.5	1249	1585.935	2313	4811
Video duration (ms)	279	118560.5	211863	589173	535475	8234399
Average bitrate (bps)	0	357145	384445	417294.6	466465	745106
Audio sample rate (Hz)	44100	44100	44100	44100	44100	44100
Audio channels	0	2	2	1.927757	2	2
Is verified	0	0	1	0.702443	1	1

Note: The derived features are not included.

2. Feature List

Data Source	Feature	Description
Webpage (Hou et al. 2019)	average_daily_view	The number of daily views of the video.
Webpage (Hou et al. 2019)	video_duration	The duration of the video.
Video (Mittal et al. 2012)	BRISQUE	A vector of 36 BRISQUE features to evaluate video quality
	chroma_stft	Compute a chromagram from a waveform or power spectrogram.
	chroma_cqt	Constant-Q chromagram.
	chroma_cens	Computes the chroma variant ‘‘Chroma Energy Normalized’’ (CENS).
	melspectrogram	Compute a mel-scaled spectrogram.
	mfcc	Mel-frequency cepstral coefficients (MFCCs).
	rms	Compute root-mean-square (RMS) value for each frame.
	spectral_centroid	Compute the spectral centroid.
	spectral_bandwidth	Compute p’th-order spectral bandwidth.
	spectral_contrast	Compute spectral contrast.
	spectral_flatness	Compute spectral flatness.
	spectral_rolloff	Compute roll-off frequency.
Acoustic (Mcfee et al. 2015)	poly_features	Coefficients of fitting a nth-order polynomial to the columns of a spectrogram.
	tonnetz	Computes the tonal centroid features (tonnetz).
	zero_crossing_rate	Compute the zero-crossing rate of an audio time series.
	tempogram	Compute the tempogram: local autocorrelation of the onset strength envelope.
	fourier_tempogram	Compute the Fourier tempogram: the short-time Fourier transform of the onset strength envelope.
	delta	Compute delta features: local estimate of the derivative of the input data along the selected axis.
	stack_memory	Short-term history embedding: vertically concatenate a data vector or matrix with delayed copies of itself.
	inverse_mel_to_stft	Approximate STFT magnitude from a Mel power spectrogram.
	inverse_mel_to_audio	Invert a mel power spectrogram to audio using Griffin-Lim.
	inverse_mfcc_to_mel	Invert Mel-frequency cepstral coefficients to approximate a Mel power spectrogram.
	inverse_mfcc_to_audio	Convert Mel-frequency cepstral coefficients to a time-domain audio signal.
	transcript_no_bigrams	The number of bi-grams.
	transcript_length	Number of terms in the transcript.
Transcript (Fernández et al. 2015, Hou et al. 2019, Liu et al. 2020)	transcript_complexity	Concentration of language and its dispersion across different terms.
	transcript_readability	How easy it is to understand the content of the video.
	transcript_informativeness	The novelty of the transcript’s terms with respect to the other posts.
	no_transcript_stats	Statistics in transcript.
	transcript_no_med_terms	The number of medical terms.
	desc_no_bigrams	The number of bi-grams.
	desc_length	Number of terms in the description.
Description (Fernández et al. 2015, Hou et al. 2019, Liu et al. 2020)	desc_complexity	Concentration of language and its dispersion across different terms.
	desc_readability	How easy it is to understand the content of the video.
	desc_informativeness	The novelty of the transcript’s terms with respect to the other posts.
	desc_no_stats	Statistics in description.
	desc_no_med_term	The number of medical terms.
	use_cipher	Whether the video uses cipher.
	allow_ratings	Whether the video allows ratings.
Webpage (Hou et al. 2019)	is_private	Whether the video is private.
	is_live_content	Whether the video is live content.
	average_bitrate	The average bitrate of the video.
	audio_sample_rate	The audio sample rate of the video.
	audio_channels	The number of audio channels of the video.
Channel (Liu et al. 2020)	content_creator_credibility	The credibility of the channel creator.
	is_verified	Whether the channel is verified.

Transcript (Fernández et al. 2015, Hou et al. 2019, Liu et al. 2020)	transcript_sentiment_neg_score	Average polarity (sentiment) of the transcript.
	transcript_sentiment_neu_score	Average polarity (sentiment) of the transcript.
	transcript_sentiment_pos_score	Average polarity (sentiment) of the transcript.
	transcript_sentiment_compound_score	Average polarity (sentiment) of the transcript.
Description (Fernández et al. 2015, Hou et al. 2019, Liu et al. 2020)	desc_sentiment_neg_score	Average polarity (sentiment) of the description.
	desc_sentiment_neu_score	Average polarity (sentiment) of the description.
	desc_sentiment_pos_score	Average polarity (sentiment) of the description.
	desc_sentiment_compound_score	Average polarity (sentiment) of the description.

3. Baseline Models

The conventional machine learning methods² include linear regression, k-nearest neighbors (KNN, using 1-nearest neighbor, 3-nearest neighbors, 5-nearest neighbors), decision tree (DT, using MSE, MAE, and Fredmanmse as the criteria), support vector regression (SVR, using linear, RBF, polynomial, and sigmoid as the kernel), and Gaussian Process. These machine learning methods are commonly adopted in continuous prediction tasks (Abbasi and Chen 2008; Arazy et al. 2016; Zhang et al. 2016). The deep learning baseline models are the most common deep learning architectures, including convolutional neural network (CNN), Long Short-Term Memory (LSTM), and Bidirectional Long Short-Term Memory (BLSTM). These models achieve state-of-the-art predictive power. However, they are blackbox models. Comparison with these models shows our method’s ability to maintain high predictive power while opening up the model to interpret the prediction. Since our method is an interpretable method, we benchmark with state-of-the-art interpretable methods, including wide and deep learning (Cheng et al. 2016), wide and deep learning with CNN (Lee and Chan 2019), wide and deep learning with LSTM (Tosun et al. 2020), wide and deep learning with BLSTM (Ye et al. 2019), and piecewise wide and deep learning (Guo et al. 2020). All the deep learning-based baseline models have the exact architecture as proposed in the referenced studies. They share the same features as our model. No feature selection or regularizations are used. We fine-tuned the hyperparameters of all the baseline models using grid search. The results reported in Tables 2-4 are the average performance of 10 times after the fine-tuning.

4. Evaluation Metrics

² KNN-*i*: *i* number of nearest neighbors; DT-MSE: decision tree with MSE as the criterion; DT-MAE: decision tree with MAE as the criterion; DT-Fredmanmse: decision tree with Fredmanmse as the criterion; SVR-Linear: SVR with linear as the kernel; SVR-RBF: SVR with RBF as the kernel; SVR-Poly: SVR with polynomial as the kernel; SVR-Sigmoid: SVR with sigmoid as the kernel; Gaussian Process-*i*: Gaussian process with the number of restarts of the optimizer as *i*.

MSE is computed using

$$\frac{1}{N} \sum_i^N (adv_i - \widehat{adv}_i)^2.$$

MAE measures the average absolute difference between the estimated values and the actual value, given by

$$\frac{1}{N} \sum_{i=1}^N |adv_i - \widehat{adv}_i|,$$

where N is the number of samples (i.e., videos). MSLE is a measure of the average squared value of the difference between logarithmic values, given by

$$\frac{1}{N} \sum_{i=1}^N (\log(1 + adv_i) - \log(1 + \widehat{adv}_i))^2.$$

MALE is similar to MSLE except that MALE measures the absolute value instead of the squared value, given by

$$\frac{1}{N} \sum_{i=1}^N |\log(1 + adv_i) - \log(1 + \widehat{adv}_i)|.$$

5. Study 1 Parameter Fine-Tuning

The average result of 10 runs is reported in following table. The results indicate using the dense layer in the higher-order component with two hidden layers and 16 neurons reaches the best performance. We use this hyperparameter setting for all the empirical analyses.

Method-Network-Layer-Neuron	MSE	MAE	MSLE	MALE
GAN-PiWAD-Dense-1-16	168.004	6.245	1.015	0.816
GAN-PiWAD-Dense-1-32	169.325	6.288	1.034	0.826
GAN-PiWAD-Dense-1-64	171.535	6.312	1.053	0.822
GAN-PiWAD-Dense-2-16	168.033	6.253	1.023	0.819
GAN-PiWAD-Dense-2-32	168.734	6.233	1.016	0.810
GAN-PiWAD-Dense-2-64	170.598	6.253	1.077	0.875
GAN-PiWAD-Dense-3-16	165.442	6.244	0.992	0.813
GAN-PiWAD-Dense-3-32	167.930	6.250	1.010	0.830
GAN-PiWAD-Dense-3-64	166.352	6.359	1.040	0.820
GAN-PiWAD-CNN-1-32	178.385	6.630	1.303	0.933
GAN-PiWAD-CNN-1-16	177.644	6.652	1.270	0.945
GAN-PiWAD-CNN-1-64	180.299	6.802	1.320	0.953
GAN-PiWAD-CNN-2-32	169.539	6.502	1.054	0.879
GAN-PiWAD-CNN-2-16	172.209	6.600	1.072	0.887

GAN-PiWAD-CNN-2-64	170.532	6.632	1.080	0.900
GAN-PiWAD-CNN-3-32	174.986	6.579	1.132	0.897
GAN-PiWAD-CNN-2-16	178.285	6.700	1.143	0.902
GAN-PiWAD-CNN-3-64	179.953	6.599	1.154	0.910
GAN-PiWAD-LSTM-1-16	175.494	6.400	1.015	0.836
GAN-PiWAD-LSTM-1-32	170.644	6.307	0.995	0.830
GAN-PiWAD-LSTM-2-16	168.650	6.299	0.984	0.815
GAN-PiWAD-LSTM-2-32	171.583	6.320	0.985	0.824
GAN-PiWAD-BLSTM-1-16	170.128	6.377	0.996	0.834
GAN-PiWAD-BLSTM-1-32	173.250	6.340	0.994	0.839
GAN-PiWAD-BLSTM-2-16	169.666	6.326	0.992	0.824
GAN-PiWAD-BLSTM-2-32	169.232	6.302	0.987	0.820

*: $p < 0.05$; **: $p < 0.01$; ***: $p < 0.001$

Note: GAN-PiWAD-CNN-1-32 is the model that uses CNN to replace the deep part of GAN-PiWAD. It has 1 hidden CNN layer with 32 neurons. Similar construction method applies to other architectures.

6. Ablation Study on Feature Groups (Study 1)

Data Sources	MSE	MAE	MSLE	MALE
All (Ours)	165.442	6.244	0.992	0.813
Without Webpage	189.535***	7.339**	1.153**	0.956**
Without Video	182.847***	7.017**	1.086**	0.928**
Without Acoustic	177.610**	6.822*	1.030	0.876*
Without Description	174.599*	6.794*	1.018	0.869*
Without Transcript	170.482*	6.583	1.004	0.851
Without Channel	170.391*	6.527	1.006	0.848

*: $p < 0.05$; **: $p < 0.01$; ***: $p < 0.001$

7. Training Results of Generative Process and VAE/Bayesian Network Ablation Results (Study 1)

The training process contains a generator and a discriminator. The learning objective is to minimize the loss of these two. The loss of the generator (G_loss) and discriminator (D_loss) in GAN-PiWAD are shown in Figure 7.1 below.

The generator loss and discriminator loss converged after 8,000 iterations, indicating the training procedure is stable. To evaluate the synthetic samples, we visualize the distributions of the synthetic samples and the real samples in Figure 7.2. Since our feature space has 854 dimensions, we reduce the dimensions to two using t-SNE for visualization purposes (Van Der Maaten and Hinton 2008). The green circles are the real samples, and the red triangles are the synthetic samples. As shown in Figure 7.2, the real samples and the synthetic samples are inseparable, suggesting the synthetic samples can accurately mimic the distribution of the real samples. This result confirms the high quality of the synthetic samples. After the generative process, GAN-PiWAD interprets how the prediction was made.

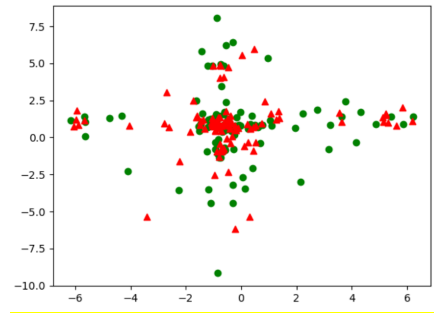
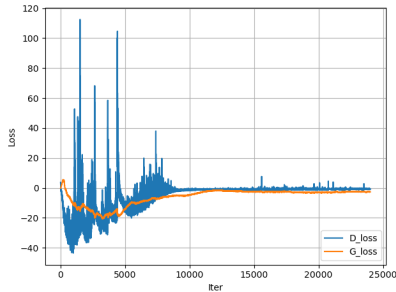


Figure 7.1. Learning Loss of the Training Process Figure 7.2. Distributions of Real and Synthetic Samples

8. The Effect of Each Feature on the Prediction (Original Values, Study 1)

Feature	GAN-PiWAD	W&D-CNN	W&D-LSTM	W&D-BLSTM	W&D	GAN-PiWAD Linear Part	Piecewise W&D
Use Cipher	0.000	0.000	0.000	0.000	0.000	0.000	0.000
Allow Ratings	0.358	-0.001	0.006	0.037	-0.310	0.659	0.296
Is Private	0.000	0.000	0.000	0.000	0.000	0.000	0.000
Is Live Content	0.539	-0.032	0.058	-0.064	0.071	0.858	0.092
Video Duration	3,166,664.753	620,196.155	-100,720.093	-133,095.685	2,465,810.515	833,088.701	2,437,884.922
Average Bitrate	-1,571.728	94,651.243	127,777.216	37,468.870	-25,962.235	-11,851.125	-5,337.014
Audio Sample Rate	44,100.000	44,100.000	44,100.000	44,100.000	44,100.000	44,100.000	44,100.000
Audio Channels	1.539	0.982	1.086	1.068	0.867	0.947	0.911
Description Bigrams	-16.097	-50.489	64.871	28.084	808.967	-674.725	-0.396
Description Length	67.984	-42.312	49.101	95.550	771.021	4,658.544	157.838
Description Complexity	0.390	-0.038	-0.039	0.024	-0.111	1.899	-0.143
Description Readability	116.890	-2.885	12.384	12.863	0.560	-468.171	34.871
Description Informativeness	3.182	-0.436	0.505	0.047	0.517	8.383	4.766
Description Stats	1.978	-1.890	7.874	5.804	106.701	15.763	0.225
Description Negative Sentiment	0.371	-0.021	0.048	0.059	0.482	1.616	-0.005
Description Neutral Sentiment	0.400	-0.058	0.009	-0.001	0.254	5.288	0.025
Description Positive Sentiment	0.146	0.034	-0.005	0.048	0.157	2.369	0.001
Description Compound Sentiment	0.379	-1.167	-0.893	-0.894	-1.329	-0.802	-1.003
Description Med Terms	269.364	-27.397	33.004	4.511	593.899	251.917	187.924
Transcript Bigrams	2,515.668	-1,733.592	108.936	1,675.324	7,066.286	-18,900.454	13,527.795
Transcript Length	1,940.411	-724.130	44.462	2,533.362	9,392.424	197.420	13,954.883
Transcript Complexity	2.503	0.173	-0.140	-0.105	-0.986	3.479	0.386
Transcript Readability	757.402	-9.944	-20.758	-40.186	168.713	-5,744.851	511.505
Transcript Informativeness	0.587	0.219	0.015	-0.005	-0.206	-1.116	-0.478
Transcript Stats	0.000	0.000	0.000	0.000	0.000	0.000	0.000
Transcript Negative Sentiment	0.784	-0.022	0.077	0.047	0.546	0.120	0.085
Transcript Neutral Sentiment	0.140	-0.030	-0.012	0.006	-0.070	0.759	0.009
Transcript Positive Sentiment	0.301	-0.079	-0.019	-0.079	-0.404	-0.882	-0.086
Transcript Compound Sentiment	0.508	-1.249	-0.970	-1.097	-2.020	-1.558	-1.601
Transcript Med Terms	440.649	-16.884	-5.740	62.037	362.382	-744.772	60.932
Content Creator Credibility	0.000	-0.026	0.108	-0.015	0.080	1.852	0.093
Is Verified	0.443	-0.072	0.141	0.080	0.704	-0.221	-0.026

9. Empirical Analyses of Study 2

Summary Statistics of Study 2

Statistic	Min	Q ₁	Median	Mean	Q ₃	Max
View count	7	1277	3135	11014.92	8070	305715
Allow ratings	0	1	1	0.991	1	1
Is live content	0	0	0	0.107	0	1
Published days	8	1075.5	1753	1935.494	2653	4629
Video duration (ms)	8893	144184	236495	515444.5	491415	8234399
Average bitrate (bps)	106759	359856	386378	426446.3	455136	741413
Audio sample rate (Hz)	44100	44100	44100	44100	44100	44100
Audio channels	1	2	2	1.91495	2	2
Is verified	0	0	1	0.637751	1	1

Note: The derived features are not included.

Hyperparameter Fine-tuning and Refining Deep Part of GAN-PiWAD (Study 2)

Method-Network-Layer-Neuron	MSE	MAE	MSLE	MALE
GAN-PiWAD-Dense-1-16	140.761	5.052	0.784	0.684
GAN-PiWAD-Dense-1-32	145.803	5.079	0.811	0.691
GAN-PiWAD-Dense-1-64	142.380	5.078	0.817	0.691
GAN-PiWAD-Dense-2-16	141.409	4.936	0.759	0.657
GAN-PiWAD-Dense-2-32	142.761	4.975	0.780	0.666
GAN-PiWAD-Dense-2-64	143.988	5.005	0.795	0.671
GAN-PiWAD-Dense-3-16	140.202	4.865	0.728	0.642
GAN-PiWAD-Dense-3-32	142.570	4.922	0.754	0.652
GAN-PiWAD-Dense-3-64	143.530	4.928	0.765	0.654
GAN-PiWAD-CNN-1-32	150.068	5.225	0.839	0.720
GAN-PiWAD-CNN-1-16	150.680	5.207	0.837	0.716
GAN-PiWAD-CNN-1-64	150.851	5.233	0.855	0.722
GAN-PiWAD-CNN-2-32	149.807	5.271	0.854*	0.727*
GAN-PiWAD-CNN-2-16	150.434	5.223	0.841	0.720
GAN-PiWAD-CNN-2-64	149.796	5.352	0.899*	0.742*
GAN-PiWAD-CNN-3-32	152.678	5.377	1.025**	0.782**
GAN-PiWAD-CNN-2-16	149.602	5.234	0.836	0.720
GAN-PiWAD-CNN-3-64	150.603	5.273	0.871*	0.727
GAN-PiWAD-LSTM-1-16	157.357*	5.179	0.828	0.730*
GAN-PiWAD-LSTM-1-32	158.520*	5.201	0.848	0.733*
GAN-PiWAD-LSTM-2-16	156.219*	5.149	0.819	0.722
GAN-PiWAD-LSTM-2-32	158.709*	5.173	0.840	0.726*
GAN-PiWAD-BLSTM-1-16	158.437*	5.202	0.849	0.733*
GAN-PiWAD-BLSTM-1-32	159.698*	5.210	0.861*	0.736*
GAN-PiWAD-BLSTM-2-16	158.132*	5.168	0.833	0.726*
GAN-PiWAD-BLSTM-2-32	158.730*	5.178	0.846	0.728*

*: $p < 0.05$; **: $p < 0.01$; ***: $p < 0.001$

Note: GAN-PiWAD-CNN-1-32 is the model that uses CNN to replace the deep part of GAN-PiWAD. It has 1 hidden CNN layer with 32 neurons. Similar construction method applies to other architectures.

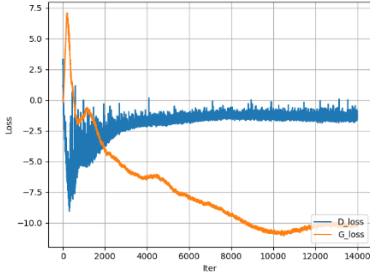
Ablation Analysis on Feature Groups by Data Source (Study 2)

Data Sources	MSE	MAE	MSLE	MALE
All (Ours)	140.202	4.865	0.728	0.642
Without Webpage	194.553***	5.575*	0.908**	0.753**
Without Video	164.936***	5.308	0.779	0.740*
Without Acoustic	155.798**	5.243	0.817*	0.717*
Without Description	156.647**	5.344	0.832*	0.658
Without Transcript	149.663*	5.121	0.770	0.667
Without Channel	147.250*	5.069	0.737	0.657

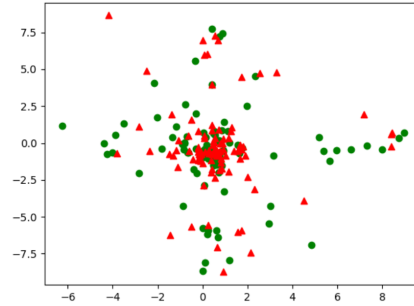
*: $p < 0.05$; **: $p < 0.01$; ***: $p < 0.001$

Dropping webpage features increases errors the most. The webpage features include the metadata about the video, such as the description. This information influences user's decision to watch the video in the first place.

Training of the Generative Process (Study 2)



Learning Loss of the Training Process



Distributions of Real and Synthetic Samples

Mean Comparison of Generative Process: WGAN-GP, VAE, and Bayesian Network (Study 2)

	Comp 1	Comp 2	Comp 3	Comp 4	Comp 5	Comp 6	Comp 7	Comp 8	Comp 9	Comp 10
Real	-2.077	-0.489	0.609	-0.220	0.046	0.030	-0.026	0.020	0.008	0.002
WGAN-GP	-2.111	-0.520	0.592	-0.230	0.042	0.028	-0.017	0.008	0.018	0.002
P-value	0.445	0.344	0.529	0.656	0.873	0.886	0.475	0.216	0.182	0.988
VAE	-2.087	-0.559	0.597	-0.215	0.016	0.002	-0.017	0.010	0.007	-0.001
P-value	0.795	0.018	0.573	0.789	0.115	0.045	0.344	0.248	0.945	0.749
Bayesian	6.274	1.568	-1.798	0.664	-0.104	-0.060	0.060	-0.038	-0.032	-0.003
P-value	0.000	0.000	0.000	0.000	0.249	0.446	0.427	0.565	0.686	0.959

Note: The p -value is the significance of t -tests comparing each model to the real samples.

The above table shows WGAN-GP and VAE can generate samples that have statistically no different means with the real samples. Bayesian Network fails to generate close sample means with the real samples.

Variation Comparison of Generative Process: WGAN-GP, VAE, and Bayesian Network (Study 2)

	Comp 1	Comp 2	Comp 3	Comp 4	Comp 5	Comp 6	Comp 7	Comp 8	Comp 9	Comp 10
Real	0.328	0.173	0.112	0.080	0.080	0.044	0.026	0.017	0.010	0.022
WGAN-GP	0.304	0.162	0.131	0.083	0.074	0.048	0.025	0.013	0.010	0.025
P-value	0.445	0.344	0.529	0.656	0.873	0.886	0.475	0.216	0.184	0.998
VAE	0.118	0.111	0.051	0.043	0.034	0.017	0.004	0.006	0.004	0.015
P-value	0.795	0.018	0.573	0.789	0.115	0.045	0.346	0.249	0.942	0.764
Bayesian	35.802	29.417	15.080	9.004	5.245	4.356	3.740	3.285	3.073	2.847
P-value	0.000	0.000	0.000	0.000	0.249	0.446	0.426	0.561	0.678	0.971

Note: The p -value is the significance of t -tests comparing each model to the real samples.

The variation comparison shows only WGAN-GP is able to generate samples that have statistically no different variations with the real samples. Considering the mean comparison and variation comparison, WGAN-GP is the best generative model in this study.

10. Factchecking Links of Misinformation Videos

Since there is limited fact-checkers for YouTube videos (most fact-checkers are for Twitter and Facebook), we use the snowball method to search for journal articles that fact-check YouTube health

videos.

No.	Link
1	https://www.newsguardtech.com/coronavirus-misinformation-tracking-center/
2	https://www.buzzfeednews.com/article/janelytvynenko/ftc-fda-scam-coronavirus-cures
3	https://ncdp.columbia.edu/microsite-page/ebola-in-perspective/ebola-myths-vs-reality/
4	https://www.nationalbreastcancer.org/breast-cancer-myths/antiperspirants-and-deodorants-cause-breast-cancer/
5	https://www.who.int/emergencies/diseases/novel-coronavirus-2019/advice-for-public/myth-busters
6	https://www.medicalnewstoday.com/articles/coronavirus-myths-explored
7	https://www.concernusa.org/story/ebola-myths-facts/
8	https://breastcancernow.org/information-support/have-i-got-breast-cancer/breast-cancer-causes/10-common-breast-cancer-myths-dispelled
9	https://theoutline.com/post/3698/insanely-popular-youtube-channel-explainer-science-fake-news?zd=1&zi=2odp534i
10	https://www.buzzfeednews.com/article/carolineodonovan/youtube-anti-vaccination-video-recommendations
11	https://www.concernusa.org/story/ebola-myths-facts/
12	https://www.wsj.com/articles/facebook-youtube-overrun-with-bogus-cancer-treatment-claims-11562072401

11. Interpretation of Study 2

As shown in Table 11.1, the description features have the most salient influence on the prediction. The description is a brief paragraph presented below a video describing an overview of the video content. This is usually the first content a viewer would read about the video, which directly influences whether the viewer will actually watch the video. The description features are the number of medical terms in the description, informativeness, readability, and complexity of the description, among others. The results show that one unit of increase in description readability results in 88.57 units of increase in average daily views. The number of medical terms has the most influence on the prediction. One unit of increase in the number of medical terms in the description will raise the average daily views by 138.69 units. These features measure how well the description can be perceived and how much medical information it contains. An easy-to-read and medically informative description leads to more transmission of health misinformation as the viewers attempt to seek medical information from the videos. Conveying the medical information that the viewers wanted to the largest extent could entertain the viewers and retain them to watch the rest of the video. If the medical information is easy to comprehend, the viewers have a better understanding of the video topic, which motivates them to watch the details from the video.

The transcript and description sentiments also significantly affect the transmission of misinformation. Notably, the negative sentiment expressed in the description and transcript has the most significant influence. A unit of increase in the description negative sentiment score (indicating stronger negative sentiment) leads to an increase of 0.36 units in average daily views. A unit of increase in the transcript

negative sentiment score increases the average daily views by 0.67 units. Negative sentiments in video content increase the transmission. In the context of health misinformation, many videos contain very emotional messages from narrators who report their experience of using medical products. For instance, some described the autism diagnosis of their children after receiving vaccination. Others reported the risk of using WiFi as they believe it is linked to coronavirus infection. The myth that eating certain food would cause cancer is also commonly shared in the misinformation videos. These negative emotions and personal narratives escalate the viewers' opposition to vaccines and food types without a factual base.

The channel features of the channel have a critical influence on the transmission as well. In particular, if a channel is verified, the transmissibility of misinformation is higher (increase the average daily views by 0.8 units). YouTube collects information from verified channels, such as phone numbers. Verified channels signal authenticity and credibility to viewers. Therefore, the viewers are more likely to watch the videos posted by these channels, regardless of whether they are misinformation or not.

Table 11.1. The Effect of Each Feature on the Prediction (Original Values, Study 2)

Features	GAN-PiWAD	GAN-PiWAD (Linear Part)	W&D	W&D-CNN	W&D-LSTM	W&D-BLSTM	Piecewise W&D
Video Duration	3459976.84	919718.50	1047090.46	420282.23	1634103.70	972748.34	-862839.13
Use Cipher	0.00	0.00	0.00	0.00	0.00	0.00	0.00
Allow Ratings	0.16	-0.67	-0.52	-0.35	-0.33	-0.26	0.00
Is Private	0.00	0.00	0.00	0.00	0.00	0.00	0.00
Is Live Content	0.52	1.78	1.25	0.69	0.66	0.42	-0.03
Average Bitrate	-2919.41	-52284.07	-41972.84	-2332.35	-82661.78	-15087.63	-60022.40
Audio Sample Rate	0.00	0.00	0.00	0.00	0.00	0.00	0.00
Audio Channels	0.38	-1.52	-1.32	-0.56	-0.66	-0.47	-0.03
Description Bigrams	88.16	3362.52	3120.55	1680.48	2068.28	2030.21	-66.90
Description Length	88.27	3362.36	3073.83	1650.12	2148.93	2073.37	-66.87
Description Complexity	0.62	-1.29	-1.09	-0.64	-0.41	-0.66	-0.15
Description Readability	88.57	80.99	98.77	44.48	86.17	59.98	-16.92
Description Informativeness	2.57	4.23	3.62	1.87	3.55	2.73	-1.02
Description Stats	12.49	323.40	276.23	168.20	188.04	188.05	-2.76
Transcript Med Terms	75.77	1973.12	1613.35	1088.01	871.60	987.59	-18.57
Description Med Term	138.69	1652.12	1654.08	930.43	1234.85	1148.01	-30.93
Transcript Bigrams	8991.50	26574.46	21770.09	17103.57	16620.70	14920.54	-1982.00
Transcript Length	6002.03	26970.81	21863.94	14609.51	14486.16	13626.26	-1959.08
Transcript Complexity	0.25	-5.90	-5.09	-0.93	-2.73	-2.38	-0.10
Transcript Readability	945.37	-1363.24	-773.65	-891.15	-448.65	-200.12	-323.32
Transcript Informativeness	1.18	3.60	2.77	2.13	1.58	1.49	-0.44
Transcript Stats	0.00	0.00	0.00	0.00	0.00	0.00	0.00
Video Feature	0.13	0.01	0.01	0.01	-0.01	0.01	-0.06
Audio Features	52.15	1.63	8.50	10.64	9.80	11.20	-15.80
Description Negative Sentiment	0.36	1.66	1.42	0.90	0.94	0.93	-0.10
Description Neutral Sentiment	0.64	1.30	1.08	0.46	0.70	0.64	-0.18
Description Positive Sentiment	0.44	0.49	0.51	0.45	0.39	0.44	-0.10
Description Compound Sentiment	-0.01	-0.14	-0.08	-0.08	-0.27	-0.05	-0.56
Transcript Negative Sentiment	0.67	2.35	2.17	1.31	0.98	0.95	-0.10
Transcript Neutral Sentiment	0.44	-0.29	-0.25	-0.20	-0.16	-0.11	-0.10
Transcript Positive Sentiment	0.29	-0.14	-0.11	-0.09	-0.10	-0.10	-0.06
Transcript Compound Sentiment	0.66	-1.35	-1.84	-0.58	-1.50	-1.05	-0.35
Content Creator Credibility	0.00	0.00	0.00	0.00	0.00	0.00	0.00
Is Verified	0.80	2.42	2.11	1.42	1.26	1.34	-0.03

The interpretation of the prediction sheds light on the management of infodemics for video platforms.

These platforms could utilize our method to monitor the description features. Medical-related videos whose description is well perceived should be under scrutiny. When a video shows overwhelmingly negative content, it needs to be closely monitored as well to prevent misinformation spread widely. Special consideration should be given to verified video channels, because their videos have a higher likelihood to transmit easily than other channels.

Our proposed method corrected the estimation error of the total effect, while the existing methods could only offer the estimation using the main effect. The error correction of our method has significant improvement on the model interpretation. For instance, in Table 11.1., our method interprets transcript readability to have a positive influence on average daily views. This is in line with the common belief since viewers are more attracted to easy-to-understand videos. However, the baseline methods interpret transcript readability to have a negative influence on average daily views. We also quantify the influence of the error correction in Table 11.2. The results suggest that the correction of estimation bias has a significant influence on the interpretation of the prediction.

Table 11.2. Influence of the Interpretation Error Correction (Normalized, Study 2)

Feature	Total effect	Main effect
Video Duration	0.42	0.11
Description Negative Sentiment	0.46	2.66
Description Neutral Sentiment	0.53	1.30
Description Positive Sentiment	0.68	0.87
Description Compound Sentiment	-0.01	-0.07
Transcript Negative Sentiment	0.24	2.35
Transcript Neutral Sentiment	0.44	-0.29
Transcript Positive Sentiment	0.08	-0.42
Transcript Compound Sentiment	0.41	-0.45
Content Creator Credibility	0.00	-0.08
Is Verified	0.80	2.42
Use Cipher	0.00	0.07
Allow Ratings	0.16	-0.67
Is Private	0.00	-0.01
Is Live Content	0.52	1.78
Average Bitrate	0.00	-0.08
Audio Sample Rate	0.00	-0.02
Audio Channels	0.48	-1.52
Description Bigrams	0.11	4.28
Description Length	0.11	4.27
Description Complexity	0.36	-1.77
Description Readability	0.25	0.68
Description Informativeness	0.39	0.56
Description Stats	0.06	6.10
Transcript Med Terms	0.05	5.25
Description Med Term	0.12	3.53
Transcript Bigrams	0.07	1.15
Transcript Length	0.26	1.16
Transcript Complexity	0.08	-1.97
Transcript Readability	0.42	-0.70
Transcript Informativeness	0.03	0.81
Transcript Stats	0.00	-0.05

Video Feature	0.34	0.03
Audio Features	0.08	0.00

To further show the difference of precise and imprecise estimations, we modify the baseline interpretable methods and add the generative process in each method. The precise total effect of each feature for the modified interpretable methods is shown in the following figure. In order to compare all the features in the same scale, we normalized the effect values. The original total effect values are reported in the following table. After modifying the baseline interpretable methods, they are able to offer precise estimation of the total effect. For each feature, the magnitude of the total effect of the baseline models is closer to GAN-PiWAD compared in that in Table 12.1. This suggests that the correction of estimation error has a significant influence on the interpretation of the prediction.

Table 11.3. Adding the GAN Component in Other Interpretable Methods (Original Value, Study 2)

Features	GAN-PiWAD	GAN-PiWAD (linear part)	GAN-W&D	GAN-W&D- CNN	GAN-W&D- LSTM	GAN-W&D- BLSTM	Piecewise W&D
Video Duration	3459976.84	919718.50	1047090.46	3987725.31	4336075.49	4950109.51	-862839.13
Use Cipher	0.00	0.00	0.00	0.00	0.00	0.00	0.00
Allow Ratings	0.16	-0.67	-0.52	0.67	0.31	0.47	0.00
Is Private	0.00	0.00	0.00	0.00	0.00	0.00	0.00
Is Live Content	0.52	1.78	1.25	0.15	0.84	0.79	-0.03
Average Bitrate	-2919.41	-52284.07	-41972.84	-2792.48	-3363.67	-4093.52	-60022.40
Audio Sample Rate	0.00	0.00	0.00	0.00	0.00	0.00	0.00
Audio Channels	0.38	-1.52	-1.32	0.00	0.46	0.00	-0.03
Description Bigrams	88.16	3362.52	3120.55	94.08	92.87	91.22	-66.90
Description Length	88.27	3362.36	3073.83	94.20	92.98	91.33	-66.87
Description Complexity	0.62	-1.29	-1.09	0.33	0.56	0.51	-0.15
Description Readability	88.57	80.99	98.77	78.25	81.22	58.55	-16.92
Description Informativeness	2.57	4.23	3.62	-0.04	-0.05	2.80	-1.02
Description Stats	12.49	323.40	276.23	41.17	11.13	15.09	-2.76
Transcript Med Terms	75.77	1973.12	1613.35	89.81	222.27	12.24	-18.57
Description Med Term	181.63	536.81	439.76	224.10	106.33	96.36	-40.04
Transcript Bigrams	6001.90	26970.22	21863.46	12035.78	10540.28	1606.70	-1959.04
Transcript Length	1949.86	-45633.95	-39364.53	6174.41	3730.13	2962.09	-778.14
Transcript Complexity	1.46	-2.10	-1.19	1.36	1.94	1.30	-0.50
Transcript Readability	514.12	1563.99	1204.05	233.38	-23.39	-28.63	-190.56
Transcript Informativeness	0.00	-0.24	0.17	0.00	0.00	0.00	-0.07
Transcript Stats	0.00	0.00	0.00	0.00	0.00	0.00	0.00
Video Feature	0.16	0.00	0.03	0.18	0.16	0.19	-0.05
Audio Features	0.17	0.81	0.69	0.21	0.23	0.22	-0.05
Description Negative Sentiment	0.40	0.81	0.67	0.26	0.28	0.34	-0.11
Description Neutral Sentiment	0.78	0.87	0.91	0.39	0.68	0.63	-0.19
Description Positive Sentiment	0.00	-0.04	-0.02	0.00	0.00	0.00	-0.16
Description Compound Sentiment	0.59	7.06	7.07	0.64	0.63	0.63	-0.13
Transcript Negative Sentiment	0.67	2.35	2.17	0.64	0.60	0.58	-0.10
Transcript Neutral Sentiment	0.44	-0.29	-0.25	0.44	0.43	0.43	-0.10
Transcript Positive Sentiment	0.29	-0.14	-0.11	0.29	0.30	0.32	-0.06
Transcript Compound Sentiment	0.66	-1.35	-1.84	1.27	0.91	0.88	-0.35
Content Creator Credibility	0.00	0.00	0.00	0.00	0.00	0.00	0.00
Is Verified	0.80	2.42	2.11	0.70	0.54	0.67	-0.03

Table 11.1. only shows the average total effect of each feature. GAN-PiWAD is also capable of estimating the dynamic total effect of each feature. Below, we randomly select four features, and show how our method captures the dynamic total effect (the dynamic total effects of average rating, channel video count, description negative sentiment, and transcript positive sentiment).

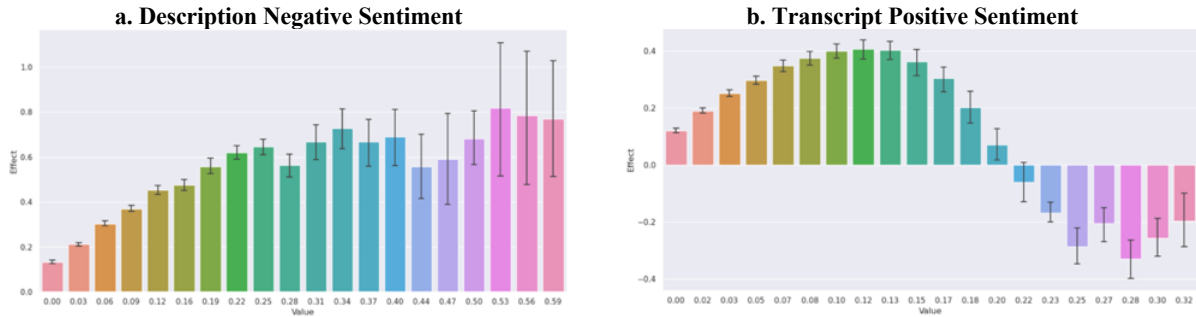


Figure 11.1. Examples of the Dynamic Total Effect (Study 2)

As suggested in the previous analyses, description negative sentiment has a salient influence on the viewership. This total effect enhances when the negative score increases, as shown in Figure 11.1.a. This happens because the strong negative sentiment in the description involves a personal connection and makes the content more relatable to the viewers. The positive sentiment of the transcript has a different dynamic effect. Figure 11.1.b. shows when the positive score is low, increasing the positive score enhances the dynamic total effect of transcript positive sentiment. This mechanism is the same as the description negative sentiment. However, when the transcript positive sentiment score is very high, its total effect on viewership turns negative. This is because an over positive video conveys a feeling of mistrust. Viewers tend to avoid those videos, which negatively affects the total effect of transcript positive sentiment.

This dynamic total effect analysis proves that the total effect of each feature is not constant. The assumption of existing studies that the prediction can be interpreted using a constant effect does not hold. The total effects could increase or decrease as the value of the feature increases. Such total effects could even turn from positive to negative and vice versa in certain situations. Dynamically interpreting the total effect is critical in predicting misinformation transmission, so that social media platforms could design more precise intervention strategies.

12. Reasons for Selecting the Models in the User Study

Model	Reason
GAN-PiWAD	Our model
W&D	Best-performing interpretable baseline model according to Table 4
Piecewise W&D	State-of-the-art model-based interpretable model
SHAP (Adding SHAP on top of our model)	State-of-the-art <i>post-hoc</i> interpretable model

VAE-based model

Test alternative interpretable component. The literature review summarized two alternatives besides GAN: VAE and Bayesian Network. We select VAE in the user study, because its generative result is better than Bayesian Network's according to Table 6 and Appendix 9.

13. User Study Full Survey

What is your age today?

Control variable: age

- Under 18
 - 18 - 24
 - 25 - 34
 - 35 - 44
 - 45 - 54
 - 55 - 64
 - 65 - 74
 - 75 - 84
 - 85 or older
-

What is your highest education level?

Control variable: education

- High school and below
 - College freshman
 - College sophomore
 - College junior
 - College senior
 - Master
 - Doctorate
-

What is your gender at birth?

Control variable: gender

- Male
 - Female
-

How knowledgeable are you in computer science?

Control variable: knowledge in CS

- Extremely knowledgeable
 - Very knowledgeable
 - Moderately knowledgeable
 - Slightly knowledgeable
 - Not knowledgeable at all
-

How knowledgeable are you in machine learning?

Control variable: knowledge in ML

- Extremely knowledgeable
- Very knowledgeable
- Moderately knowledgeable
- Slightly knowledgeable
- Not knowledgeable at all

How often do you watch video sharing websites, such as YouTube, Vimeo, Bilibili, YouKu, and iQiyi?

Control variable: video viewing frequency

- Everyday
- A few times a week
- Once a week
- A few times a month
- Never

Have you ever uploaded videos to video sharing websites, such as YouTube, Vimeo, Bilibili, YouKu, and iQiyi?

Control variable: uploading experience

- Yes
- No

How do you agree with the following statement?

"I trust artificial intelligence and automation." Control variable: trust in AI and automation

- Strongly agree
- Somewhat agree
- Neither agree nor disagree
- Somewhat disagree
- Strongly disagree

On a scale of the easiest to the most difficult, how difficult is it for you to do the following?

Control variable: health literacy (Osborne et al. 2013)

	Extremely easy	Somewhat easy	Neither easy nor difficult	Somewhat difficult	Extremely difficult
Understand advice on health from family members or friends	<input type="radio"/>	<input type="radio"/>	<input type="radio"/>	<input type="radio"/>	<input type="radio"/>
Understand information on food packaging	<input type="radio"/>	<input type="radio"/>	<input type="radio"/>	<input type="radio"/>	<input type="radio"/>
Understand information in the media on how to get healthier	<input type="radio"/>	<input type="radio"/>	<input type="radio"/>	<input type="radio"/>	<input type="radio"/>
Understand information on how to keep your mind healthy	<input type="radio"/>	<input type="radio"/>	<input type="radio"/>	<input type="radio"/>	<input type="radio"/>



In this survey, we will show you a YouTube video about health information. You will be asked to **predict the daily viewership of this video (How many times on average this video will be watched in a day). The more accurate your prediction is, the higher your compensation will be.**

To assist your prediction on video viewership, we will provide you a machine learning model. We will show you the variables that this model uses and the weights of the variables. The more reasonable variables and weights will achieve better prediction performance.

Variables are information related to the audio and video, such as video quality, audio sentiment, medical knowledge in the video, etc.

Different variables carry different weights in the machine learning model. Higher weight indicates this variable has a higher influence on the prediction (of the daily viewership of YouTube videos). Positive weight indicates this variable positively influences the prediction, and vice versa.

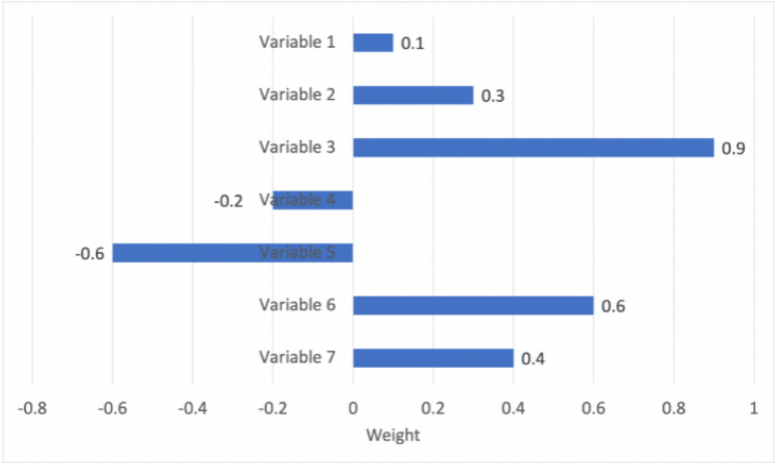
Survey instruction



Here is an example to help you understand the task. Below is a machine learning model that can predict the daily viewership of YouTube videos. This model uses variables 1-7 to predict the daily viewership. In the below figure, the vertical axis shows these variables. The horizontal axis shows the weight of each variable.

Training

The length of the bar indicates the weight of each variable in the prediction. The weight value is also shown at the end of the bar. For instance, if the weight of a variable is 0.3, this means increasing this variable by 1 unit, the model will predict this video's daily viewership will increase by 0.3 units.



According to the above figure, when using the above model to predict the daily viewership of videos, what are the top two essential variables that have positive effects?

Training test question 1

- Variable 1
- Variable 2
- Variable 3
- Variable 4
- Variable 5
- Variable 6
- Variable 7

According to the weights in the figure, if variable 6 increases by 1 unit, how will the above model prediction of video viewership change?

Training test question 2

- Increase by 0.3 unit
- Increase by 0.6 unit
- Decrease by 0.3 unit
- Decrease by 0.6 unit



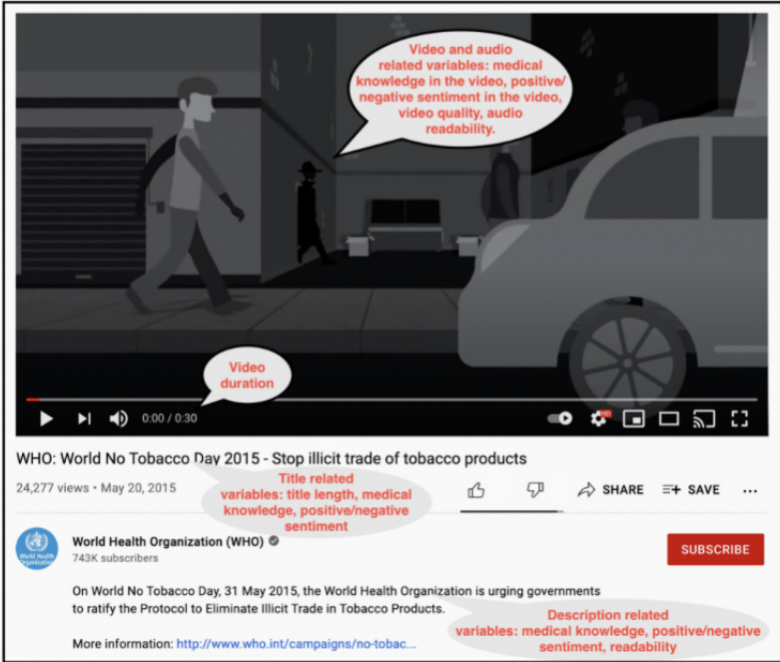
Please watch this YouTube video, then answer the following questions:



Video

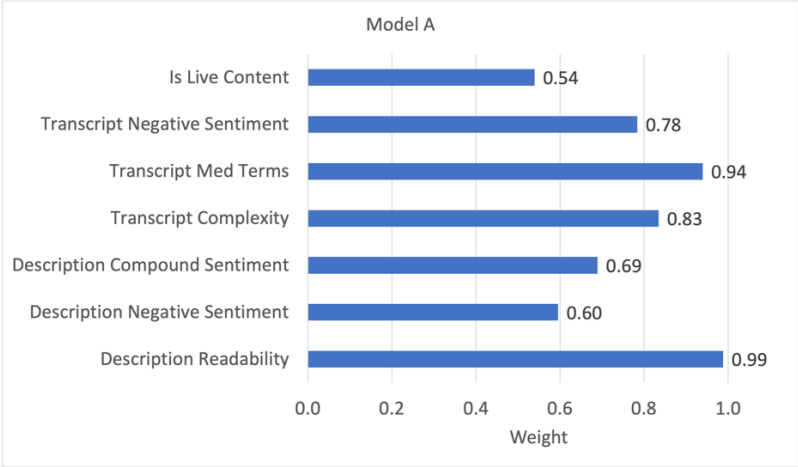
Now we provide you with a machine learning model (Model A) to predict the viewership of the above video. Many variables can be extracted from this video. Some of them are shown in the following screenshot (red words).

Video webpage screenshot with variable notations



Our research team built your assigned model (Model A) based on the deep learning framework. This model was trained on 10,000 YouTube videos. It learned to extract information from the video and predict the daily viewership. In this task, your model selected 7 most important variables for the viewership prediction task. These variables are shown in the vertical axis in the following figure. The horizontal axis indicates the weight of the variables in the model.

Model display



According to the above figure, when using the above model (Model A) to predict video viewership, please rank the following variables from the most important to the least important used by the model. Please put the most important variable on the top and the least important on the bottom. You can drag the variables to reorder.

Model test question 1

Hint: The importance of a variable in a prediction can be measured by the weight of the variable.

Is live content
Transcript negative sentiment
Transcript med terms
Transcript complexity
Description compound sentiment
Description negative sentiment
Description readability

What are the top 2 most essential variables in the above model?

Model test question 2

- Description readability
- Description negative sentiment
- Transcript med terms
- Transcript complexity

If the creator of the above video would like to increase video viewership, which of the following option is more effective?

Model test question 3

- Increase "Is live content" by 1 unit
- Increase "Transcript negative sentiment" by 1 unit

According to the weights in the figure, if the "Description negative sentiment" increases by 1 unit, how will the above model prediction of video viewership change?

Model test question 4

- Increase by 1 unit
- Increase by 0.6 unit
- Decrease by 1 unit
- Decrease by 0.6 unit



More reasonable ranking and weights of variables result in better prediction performance. Do you think the ranking and weights of the variables in the model in the previous page are reasonable? How much do you trust the model in the previous page in predicting the daily viewership of YouTube videos? Please answer these questions by rating the following statements. The ranking and weights of variables of this model is shown again in the bottom (The variables are ranked by their importance).

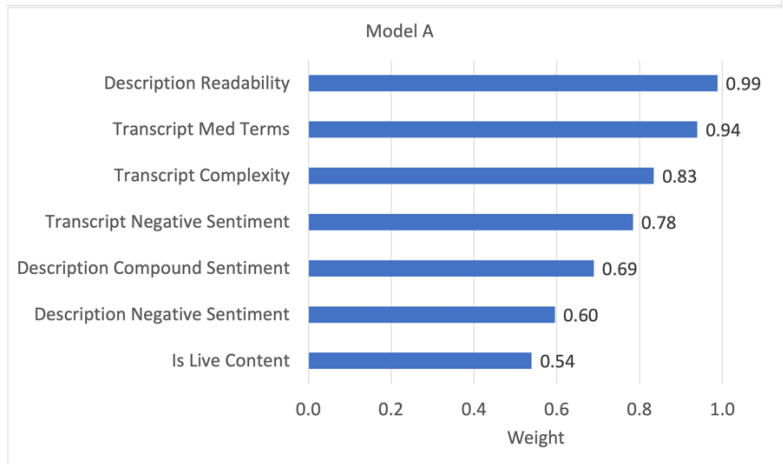
Interpretability measurement 1: trust in automated systems (Jian et al. 2000; Chai et al. 2011)

	Strongly agree	Somewhat agree	Neither agree nor disagree	Somewhat disagree	Strongly disagree
The model is deceptive	<input type="radio"/>	<input type="radio"/>	<input type="radio"/>	<input type="radio"/>	<input type="radio"/>
The model behaves in an underhanded manner	<input type="radio"/>	<input type="radio"/>	<input type="radio"/>	<input type="radio"/>	<input type="radio"/>
I am suspicious of the model's intentions, action, or outputs	<input type="radio"/>	<input type="radio"/>	<input type="radio"/>	<input type="radio"/>	<input type="radio"/>
I am wary of the model	<input type="radio"/>	<input type="radio"/>	<input type="radio"/>	<input type="radio"/>	<input type="radio"/>
Please just select "Neither agree nor disagree"	<input type="radio"/>	<input type="radio"/>	<input type="radio"/>	<input type="radio"/>	<input type="radio"/>
I am confident in the model	<input type="radio"/>	<input type="radio"/>	<input type="radio"/>	<input type="radio"/>	<input type="radio"/>
The model has integrity	<input type="radio"/>	<input type="radio"/>	<input type="radio"/>	<input type="radio"/>	<input type="radio"/>
The model is dependable	<input type="radio"/>	<input type="radio"/>	<input type="radio"/>	<input type="radio"/>	<input type="radio"/>
The model is reliable	<input type="radio"/>	<input type="radio"/>	<input type="radio"/>	<input type="radio"/>	<input type="radio"/>
I can trust the model	<input type="radio"/>	<input type="radio"/>	<input type="radio"/>	<input type="radio"/>	<input type="radio"/>

We are interested in studying how useful this model is in predicting the daily viewership of a video. Please consider the below picture. If we show you the values of the seven variables of the video in the previous page, how useful is Model A in assisting your prediction, compared to no model assistance? Please rate the following statement.

Interpretability measurement 2: usefulness (Davis 1989; Davis et al., 1989; Adams et al. 1992)

	Strongly agree	Somewhat agree	Neither agree nor disagree	Somewhat disagree	Strongly disagree
Using this model allows me to accomplish the prediction more quickly.	<input type="radio"/>	<input type="radio"/>	<input type="radio"/>	<input type="radio"/>	<input type="radio"/>
Using this model enhances my effectiveness on the prediction.	<input type="radio"/>	<input type="radio"/>	<input type="radio"/>	<input type="radio"/>	<input type="radio"/>
Using this model improves my prediction performance	<input type="radio"/>	<input type="radio"/>	<input type="radio"/>	<input type="radio"/>	<input type="radio"/>
Please just select "Neither agree nor disagree"	<input type="radio"/>	<input type="radio"/>	<input type="radio"/>	<input type="radio"/>	<input type="radio"/>
Using this model makes it easier to do my prediction.	<input type="radio"/>	<input type="radio"/>	<input type="radio"/>	<input type="radio"/>	<input type="radio"/>
Overall, I find using this model to be advantageous in my prediction.	<input type="radio"/>	<input type="radio"/>	<input type="radio"/>	<input type="radio"/>	<input type="radio"/>
Using this model increases my productivity.	<input type="radio"/>	<input type="radio"/>	<input type="radio"/>	<input type="radio"/>	<input type="radio"/>



Now you have a chance to decide whether you want to keep the current model. If you think the variables and weights of the previous model (Model A) are not reasonable, you have a chance to change to a different model. If you are satisfied with the current model, you can keep the current model.

[Instruction on changing model](#)

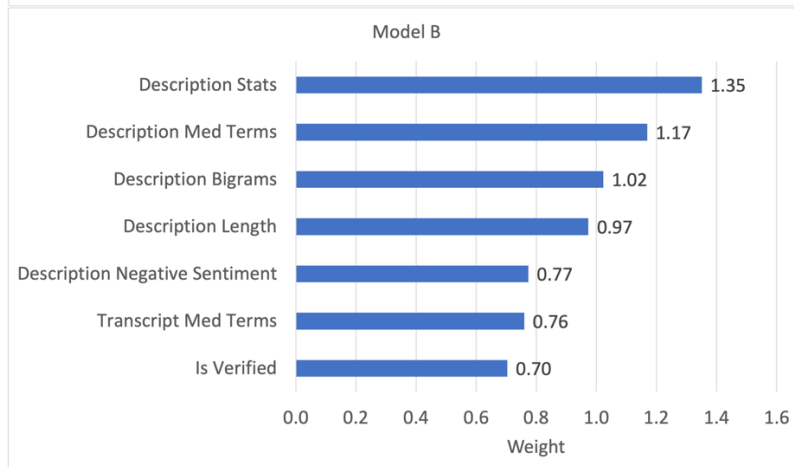
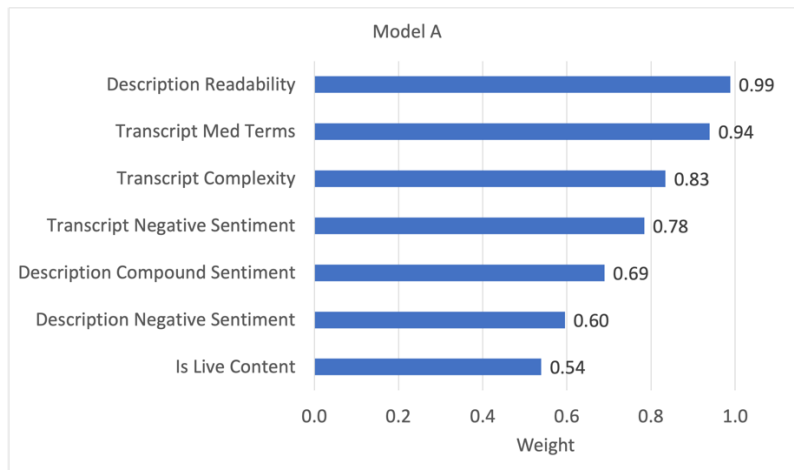
Please note: **Your compensation is positively related to the prediction performance. The better the prediction performance, the higher your compensation. More reasonable variables and weights lead to better performance.**

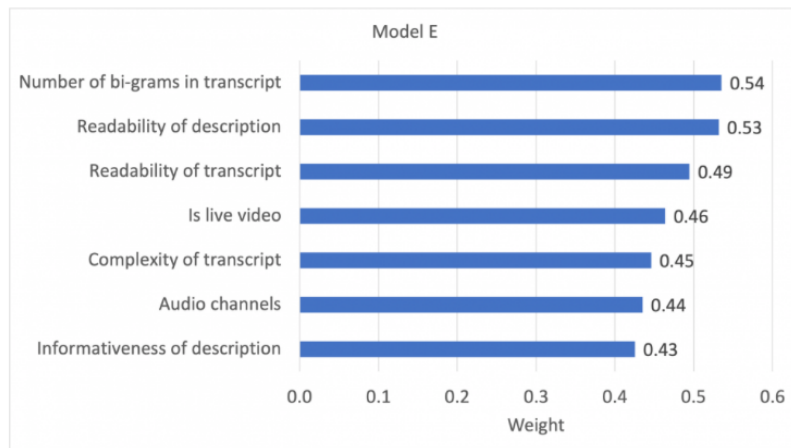
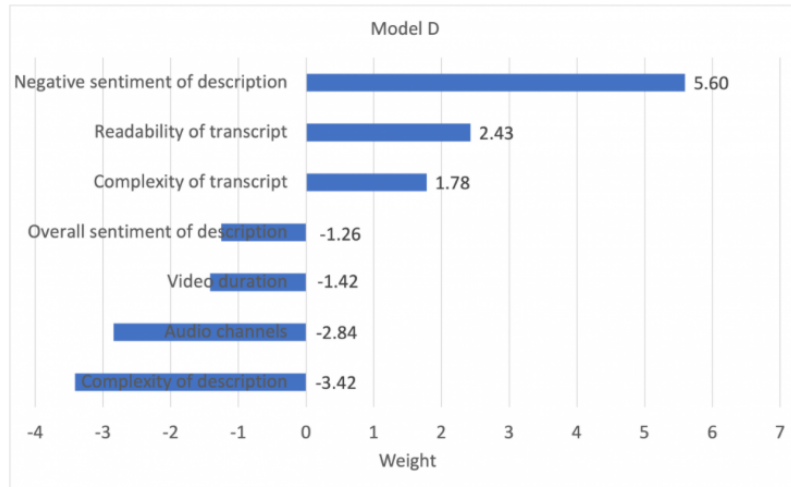
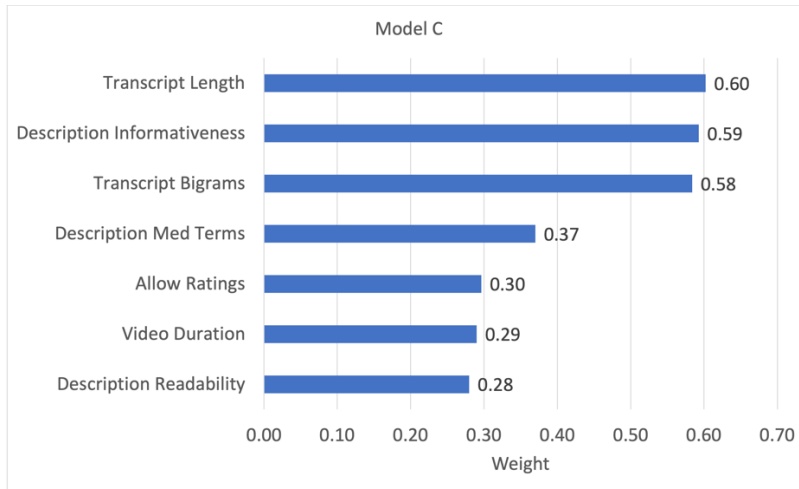
You will see your current model as well as four alternative models in the next page. You can compare the variables used in the model and their weights, then decide whether you would like to keep the current model or change to a different one.



Below are five models. Their variables and weights are different. Model A is your current model shown in the previous pages. The other four models are alternatives. The variables are shown in the vertical axis in the following figure. The horizontal axis indicates the weight of the variables in the model.

[Display of all models \(Order is randomized\)](#)





In order to make the most accurate viewership prediction, please decide whether you would like to keep the current model or change to an alternative model. Your decision should base on which model has the most reasonable variables and weights. Final model adoption

Hint: When the choice of variables, variable ranking, and variable weights are more reasonable, the model prediction performance is better. Which model would you like to choose?

- Model A
- Model B
- Model C
- Model D
- Model E

Now consider the model you just chose. Do you think the ranking and weights of the variables in this model are reasonable? How much do you trust this model in predicting the daily viewership of YouTube videos? Please answer these questions by rating the following statements. If you chose an alternative model, please rate the new model. If you kept the same model, please rate this model again.

Interpretability measurement 1: trust in automated systems (Jian et al. 2000; Chai et al. 2011)

	Strongly agree	Somewhat agree	Neither agree nor disagree	Somewhat disagree	Strongly disagree
The model is deceptive	<input type="radio"/>	<input type="radio"/>	<input type="radio"/>	<input type="radio"/>	<input type="radio"/>
The model behaves in an underhanded manner	<input type="radio"/>	<input type="radio"/>	<input type="radio"/>	<input type="radio"/>	<input type="radio"/>
I am suspicious of the mode's intentions, action, or outputs	<input type="radio"/>	<input type="radio"/>	<input type="radio"/>	<input type="radio"/>	<input type="radio"/>
I am wary of the model	<input type="radio"/>	<input type="radio"/>	<input type="radio"/>	<input type="radio"/>	<input type="radio"/>
Please just select "Neither agree nor disagree"	<input type="radio"/>	<input type="radio"/>	<input type="radio"/>	<input type="radio"/>	<input type="radio"/>
I am confident in the model	<input type="radio"/>	<input type="radio"/>	<input type="radio"/>	<input type="radio"/>	<input type="radio"/>
The model has integrity	<input type="radio"/>	<input type="radio"/>	<input type="radio"/>	<input type="radio"/>	<input type="radio"/>
The model is dependable	<input type="radio"/>	<input type="radio"/>	<input type="radio"/>	<input type="radio"/>	<input type="radio"/>
The model is reliable	<input type="radio"/>	<input type="radio"/>	<input type="radio"/>	<input type="radio"/>	<input type="radio"/>
I can trust the model	<input type="radio"/>	<input type="radio"/>	<input type="radio"/>	<input type="radio"/>	<input type="radio"/>

How useful is this model in assisting your prediction, compared to no model assistance? Please rate the following statement. If you chose an alternative model, please rate the new model. If you kept the same model, please rate this model again.

Interpretability measurement 2: usefulness (Davis 1989; Davis et al., 1989; Adams et al. 1992)

	Strongly agree	Somewhat agree	Neither agree nor disagree	Somewhat disagree	Strongly disagree
Using this model allows me to accomplish the prediction more quickly.	<input type="radio"/>	<input type="radio"/>	<input type="radio"/>	<input type="radio"/>	<input type="radio"/>
Using this model enhances my effectiveness on the prediction.	<input type="radio"/>	<input type="radio"/>	<input type="radio"/>	<input type="radio"/>	<input type="radio"/>
Using this model improves my prediction performance	<input type="radio"/>	<input type="radio"/>	<input type="radio"/>	<input type="radio"/>	<input type="radio"/>
Please just select "Neither agree nor disagree"	<input type="radio"/>	<input type="radio"/>	<input type="radio"/>	<input type="radio"/>	<input type="radio"/>
Using this model makes it easier to do my prediction.	<input type="radio"/>	<input type="radio"/>	<input type="radio"/>	<input type="radio"/>	<input type="radio"/>
Overall, I find using this model to be advantageous in my prediction.	<input type="radio"/>	<input type="radio"/>	<input type="radio"/>	<input type="radio"/>	<input type="radio"/>
Using this model increases my productivity.	<input type="radio"/>	<input type="radio"/>	<input type="radio"/>	<input type="radio"/>	<input type="radio"/>

Note:

The red notations on the upper right corner are just for explanatory purpose in this appendix. They are not displayed in the survey.

The medical literacy scale is adopted from:

Osborne RH, Batterham RW, Elsworth GR, Hawkins M, Buchbinder R. The grounded psychometric development and initial validation of the Health Literacy Questionnaire (HLQ). BMC public health. 2013 Dec;13(1):1-7.

The trust in automated systems scale is adopted from:

Jian JY, BisantzAM, Drury CG. Foundations for an empirically determined scale of trust in automated systems. International journal of cognitive ergonomics. 2000 Mar 1;4(1):53-71.

Chai S, Das S, Rao HR. Factors affecting bloggers' knowledge sharing: An investigation across gender. Journal of Management Information Systems. 2011 Dec 1;28(3):309-42

The usefulness scale is adopted from:

Davis FD. Perceived usefulness, perceived ease of use, and user acceptance of information technology. MIS quarterly. 1989 Sep 1:319-40.

Davis FD, Bagozzi RP, Warshaw PR. User acceptance of computer technology: A comparison of two theoretical models. Management science. 1989 Aug;35(8):982-1003.

Adams DA, Nelson RR, Todd PA. Perceived usefulness, ease of use, and usage of information technology: A replication. MIS quarterly. 1992 Jun 1:227-47.

14. Summary Statistics of Control Variables in User Study

Age	Number
18 - 24	107
25 - 34	43
35 - 44	1
55 - 64	1
Gender	Number
F	77
M	75
Education	Number
Freshmen	2
Sophomore	22
Junior	37
Senior	31
Master	41
Doctorate	19

Variable	Min.	1st quartile	Median	Mean	3rd quartile	Max.
CS Knowledge	1.00	2.00	3.00	2.70	3.00	4.00
ML Knowledge	1	2	3	2.586	3	4
Video Watching Frequency	1	3	3	3.132	4	4
Upload Experience	0	0	0	0.09211	0	1
Trust in AI	1	2	3	2.842	3	4
Health Literacy	1.75	2.5	3	3.012	3.5	4

Note: After removing incomplete responses and those who failed the attention check, we collected 152 responses. The attention check can be found in the trust in automated systems scale in Appendix 12.

15. Randomization Check in User Study

Variable	<i>P</i> -value of ANOVA (Interpretability: Trust)	<i>P</i> -value of ANOVA (Interpretability: Usefulness)
Age	0.281	0.404
Education	0.265	0.349
Gender	0.449	0.133
CS Knowledge	0.884	0.944
ML Knowledge	0.335	0.410
Video Watching Frequency	0.602	0.973
Upload Experience	0.811	0.589
Trust in AI	0.579	0.560
Health Literacy	0.306	0.213

Note: As discussed in the paper, we adopt two measurements for ML interpretability: trust in automated systems (Chai et al. 2014, Jian et al. 2010) and model usefulness (Dhurandhar et al. 2017, Lee et al. 2018).

16. User Study Training Session Error Message

Incorrect answer. Please choose again. Hint: pay attention to the weight of the variables.

According to the weights in the figure, if variable 6 increases by 1 unit, how will the above model prediction of video viewership change?

- Increase by 0.3 unit
- Increase by 0.6 unit
- Decrease by 0.3 unit
- Decrease by 0.6 unit

17. User Study Video Webpage Screenshot

18. User Study Error Message

Incorrect answer. Please choose again. Hint: pay attention to the weight of the variables.

According to the above figure, when using the above model (Model A) to predict video viewership, please rank the following variables from the most important to the least important used by the model. Please put the most important variable on the top and the least important on the bottom. You can drag the variables to reorder.

Hint: The importance of a variable in a prediction can be measured by the weight of the variable.

- 1 Is live content
- 2 Transcript negative sentiment
- 3 Transcript med terms
- 4 Description compound sentiment
- 5 Transcript complexity
- 6 Description negative sentiment
- 7 Description readability

19. Reliability and Validity of Interpretability Scale

Interpretability: Trust (Cronbach's Alpha = 0.963)	Factor loading
Trust 1	0.805
Trust 2	0.701
Trust 3	0.866
Trust 4	0.872
Trust 5	0.911
Trust 6	0.903
Trust 7	0.908
Trust 8	0.925
Trust 9	0.892

Interpretability: Usefulness (Cronbach's Alpha = 0.975)	Factor loading
Usefulness 1	0.939
Usefulness 2	0.935
Usefulness 3	0.934
Usefulness 4	0.934
Usefulness 5	0.913
Usefulness 6	0.940

The trust in automated systems scale is adopted from:

Jian JY, BisantzAM, Drury CG. Foundations for an empirically determined scale of trust in automated systems. International journal of cognitive ergonomics. 2000 Mar 1;4(1):53-71.

Chai S, Das S, Rao HR. Factors affecting bloggers' knowledge sharing: An investigation across gender. Journal of Management Information Systems. 2011 Dec 1;28(3):309-42

The usefulness scale is adopted from:

Davis FD. Perceived usefulness, perceived ease of use, and user acceptance of information technology. *MIS quarterly*. 1989 Sep 1:319-40.

Davis FD, Bagozzi RP, Warshaw PR. User acceptance of computer technology: A comparison of two theoretical models. *Management science*. 1989 Aug;35(8):982-1003.

Adams DA, Nelson RR, Todd PA. Perceived usefulness, ease of use, and usage of information technology: A replication. *MIS quarterly*. 1992 Jun 1:227-47.

References

Abbasi A, Chen H (2008) CyberGate: a design framework and system for text analysis of computer-mediated communication. *MIS Q.* 32(4):811–837.

Arazy O, Daxenberger J, Lifshitz-Assaf H, Nov O, Gurevych I (2016) Turbulent Stability of Emergent Roles: The Dualistic Nature of Self-Organizing Knowledge Coproduction. *Inf. Syst. Res.* 27(4):792–812.

Cheng HT, Koc L, Harmsen J, Shaked T, Chandra T, Aradhya H, Anderson G, et al. (2016) Wide & deep learning for recommender systems. *ACM Int. Conf. Proceeding Ser.* 7–10.

Fernández M, Burel G, Alani H, Piccolo LSG, Meili C, Hess R (2015) Analysing engagement towards the 2014 Earth Hour Campaign in Twitter. *EnviroInfo & ICT4S 2015 Build. Knowl. Base Environ. Action Sustain.*

Guo M, Zhang Q, Liao X, Zeng DD (2020) An interpretable neural network model through piecewise linear approximation.

Hou R, Pérez-Rosas V, Loeb S, Mihalcea R (2019) Towards Automatic Detection of Misinformation in Online Medical Videos. *Proc. 2019 Int. Conf. Multimodal Interact.:*235–243.

Lee JW, Chan YY (2019) Fine-Grained Plant Identification using wide and deep learning model. *2019 Int. Conf. Platf. Technol. Serv. PlatCon 2019 - Proc.*

Liu X, Zhang B, Susarla A, Padman R (2020) Go to YouTube and Call Me in the Morning: Use of Social Media for Chronic Conditions. *MIS Q.*

Mcfee B, Raffel C, Liang D, Ellis DPW, Mcvicar M, Battenberg E, Nieto O (2015) librosa: Audio and Music Signal Analysis in Python. *PROC. 14th PYTHON Sci. CONF.*

Mittal A, Moorthy AK, Bovik AC (2012) No-reference image quality assessment in the spatial domain. *IEEE Trans. Image Process.* 21(12):4695–4708.

Tosun N, Sert E, Ayaz E, Yilmaz E, Gol M (2020) Solar Power Generation Analysis and Forecasting Real-World Data Using LSTM and Autoregressive CNN. 1–6.

Ye H, Cao B, Peng Z, Chen T, Wen Y, Liu J (2019) Web Services Classification Based on Wide & Bi-LSTM Model. *IEEE Access* 7:43697–43706.

Zhang D, Zhou L, Kehoe JL, Kilic IY (2016) What Online Reviewer Behaviors Really Matter? Effects of Verbal and Nonverbal Behaviors on Detection of Fake Online Reviews. *J. Manag. Inf. Syst.* 33(2):456–481.